To the Graduate Council:

I am submitting herewith a thesis written by D. Dewayne Foust entitled "Column Evaporation Study Conducted on Fly Ash for the Evaluation of Evaporation Routines of Three Numerical Water Budget Models." I have examined the final copy of this thesis for form and content and recommend that it be accepted in partial fulfillment of the requirements for the degree of Masters of Science, with a major in Environmental Engineering.

Dr. B. A. Tschantz, Major Professor

We have read the thesis
and recommend its acceptance:

James L. Smoot

Wayne T. Davis

Accepted for the council:

C W Minkel

Associate Vice Chancellor
and Dean of The Graduate School

STATEMENT OF PERMISSION TO USE

In presenting this thesis in partial fulfillment of the requirements for a Master's degree at the University of Tennessee, Knoxville, I agree that the Library shall make it available to borrowers under rules of the Library. Brief quotations from this thesis are allowable without special permission, provided that accurate acknowledgment of the source is made.

Requests for permission for extensive quotation from or reproduction of this thesis in whole or in parts may be granted by the copyright holder.

Signature D. Dewayne Foust

Date 4/30/92

Column Evaporation Study Conducted on Fly Ash for the Evaluation of Evaporation Routines of Three Numerical Water Budget Models

A Thesis

Presented for the

Master of Science

Degree

The University of Tennessee, Knoxville

D. Dewayne Foust

May 1992

ACKNOWLEDGEMENTS

This study was sponsored by the Tennessee Valley Authority (TVA) while I was working as a graduate research assistant at the Norris Engineering Laboratory.

I would like to recognize individuals at TVA for their contributions to this thesis project:

- Steve Young for guiding the research;
- Hubert Pearson and Charles Savas for providing laboratory equipment and facilities;
- Hank Julian and Linda Smith for technical and graphical support;
- Catherine Patty and Karen Miller for word processing and copying articles;
- Cynthia Webb for editing the manuscript

I would like to recognize the Graduate Committee (Dr. Wayne Davis, Dr. James Smoot, and Dr. Bruce Tschantz) for the comments and helpful criticism. I especially would like to thank B. A. Tschantz for his help and cooperation as my major professor.

Finally, I am thankful for the patience and understanding my wife has shown throughout my graduate work.

ABSTRACT

Results from a fly ash column evaporation study were compared to computer-simulated values of HELP2, UNSAT1D, and the Wetting Front model. All three models used the same input data. The Wetting Front model showed the best agreement between the experimental value and the computed values, within 6.3% for Colbert fly ash and 5.4% for Kingston fly ash. Modeled results for HELP2 and UNSAT1D showed a range difference of 53 to 36% and 95 to 97% respectively, for Colbert and Kingston fly ash.

Default values used by the HELP2 model when compared to fly ash suggested that differences between fly ash and soils existed. These differences were shown as the evaporation coefficients.

As a result of the column evaporation study, codes that simulate soil-water movement should be analyzed before they are used to estimate the water budget of fly ash. Based on the comparison of cumulative evaporation between actual measured data and modeled data, codes derived from the Richards equation had an advantage over other models developed from empirical equations based on field studies.

TABLE OF CONTENTS

CONTENTS
(Continued)

FIGURES

LIST OF TABLES

1.0 INTRODUCTION

1.1 Basis for Study

The Tennessee Valley Authority (TVA) has 11 fossil plants that are used to produce power for the Tennessee Valley. Under normal operations, these plants use low sulfur coal (2% or less) as the primary combustion source. As a result of this combustion process, large amounts of secondary waste ($2x10^6$ tons annually) are produced. This secondary waste, known as fly ash, is a solid residue that consists of inorganic mineral constituents and organic matter which is not fully burned during coal combustion.

Until recently the waste has been disposed of by using water to transport the ash via canal or pipeline to waste ponds. This type of disposal method requires considerable space and has the potential for groundwater contamination as a result of leachate problems. The amount of leachate produced from ponded fly ash is primarily controlled by water levels in the pond. Due to the presence of potentially hazardous constituents in the fly ash, TVA, the Environmental Protection Agency (EPA), and the Tennessee Department of Environment and Conservation have expressed concerns about contamination of ground water from leachate migration.

To help reduce space for disposal and decrease the quantity of leachate produced, TVA has recently converted to a new disposal technique known as dry stacking. Since dry stacking requires the ash to be compacted, the storage volume is reduced. A key element of the overall assessment of the design and potential environmental impact is the prediction of the quantity of waste leachate produced as a result of infiltration of precipitation through the waste stack.

Because of the small particle size, fly ash exhibits strong capillary forces that tend to prevent drainage but promote evaporation (Young 1989). Therefore, in order to accurately predict leachate quantities it is necessary to determine evaporation. A numerical model capable of providing accurate predication is desirable.

A numerical water budget model typically requires several simplifying assumptions, each of which distracts from the ability of the model to portray the actual prototype. It is usually recognized that the accuracy of a model is only as good as the data that goes into it. However, for the results to be considered, acceptable knowledge of the model's application is needed. This study focuses on evaluating the evaporation routine of three numerical water budget models.

A column evaporation study provided the experimental data necessary to evaluate the model results. The models used in the study were the 1-dimensional unsaturated flow models UNSAT1D (Bond, et al., 1984), Hydraulic Evaluation Landfill Performance Version 2 (HELP2) (Shroeder, et al., 1984), and the Wetting Front (WF) Model (Clapp, 1982). These models were used to simulate evaporation based on the meteorological conditions of the experiment and hydraulic properties of the fly ash.

1.2 Background

In 1949, increasing power demands from consumers prompted TVA to begin building a series of large coal-fired power plants, which now account for about 69% of TVA's power-generating capacity. The combustion of coal results in a variety of products of complete and incomplete combustion. The most common products are bottom ash and fly ash. Generally, for TVA fossil plants, the ash consists of approximately 85% fly ash and 15% bottom ash.

Fly ash is a solid residue that consists primarily of inorganic mineral constituents and organic matter that is not fully consumed during coal combustion. The major constituents of the ash are silicon, aluminum, iron, and calcium. Typically, these constituents comprise about 95 to 99% by weight of fly ash. Minor constituents, such as magnesium, titanium, sodium, potassium, sulfur, and phosphorus, comprise 0.5 to 3.5% (Young and Beard, 1989). The chemical composition of fly ash depends on the characteristics of the coal and can vary for different types of coal.

For disposal, dry ash is transported in 30 to 40 ton loads by truck to a designated stacking area. The ash is then dumped and spread over the disposal area in 10 to 16-cm lifts. Moisture is added to the dry ash to obtain optimum compaction and to reduce problems with fugitive dust. The optimum compaction rate usually occurs at a gravimetric moisture content between 18 and 24%. The active dry stack is compacted and sloped approximately three to four % to minimize erosion.

Because land disposal facilities require permits from state and/or federal regulatory agencies, a good understanding of potential groundwater contamination concerns is an important issue. A major consideration is the potential amount of leachate produced from dry stacking. From a study conducted at Colbert Fossil Plant, Lindquist and Young (1990) presented evidence that dry stacking produces less than one-tenth of the total quantity of leachate produced by wet-sluicing. Additional field research performed on dry stacking by Young (1989) addressed the components of the water budget for analysis of leachate at the Bull Run disposal site. Based on the results of the investigation, the leachate from the active fly ash dry stack was estimated to be between zero and five % of the total rainfall. The small amount of leachate was attributed mainly to the high evaporation capacity of the dry-stacked ash. It is important to estimate quantities of leachate in order to validate the success of the disposal technique and improve the design of disposal areas.

1.3 Purpose and Scope of Study

Three water budget models have been developed that are potentially capable of predicting the two-staged evaporation process through partially saturated media. The models are UNSAT1D, HELP2, and the Wetting Front Model. However, these models have not been validated for fly ash, which leaves doubt as to the reliability of their predictions. The goal of this project was to develop data for model validation through a controlled study and to utilize this data to evaluate the models' ability to predict evaporation from fly ash. The principal objectives of the study were to:

1. Perform controlled experiments to determine the evaporation rate from fly ash collected at the Colbert and Kingston Fossil Plants.

2. Review soil-water concepts and the evaporation process as related to the algorithm of the computer models.

3. Determine the evaporation coefficient for Colbert and Kingston fly ash.

4. Compare and evaluate outputs from the three numerical models to measured experimental values for Colbert and Kingston fly ash.

2.0 SOIL-WATER REVIEW

2.1. Background

In order to interpret the models, it is beneficial to describe concepts of soil-water and soil moisture movement as related to evaporation. The concept of staged evaporation used by the models required moisture from the evaporating surface to be removed, thus creating a gradient resulting in the upward movement of moisture in the porous media. This chapter defines soil terms, addresses parameters that impact soil-water movement (vertical), and describes the evaporation process. Besides describing the flow process to the surface, governing equations and addition factors are also considered.

2.2 Soil Moisture

In soils, water is held in the pore space commonly defined as porosity or void ratio. Porosity is an index of pore volume in a given soil sample, represented as:

$$n = \frac{V_p}{V_T} \tag{1}$$

where:

n = porosity (dimensionless)
V_p = volume of the pores (cm^3)
V_T = total volume (cm^3)

The void ratio is also an index, but it relates the pore volume to the volume of pore solids, given as:

$$e = \frac{V_p}{V_s} \tag{2}$$

where:

e = void ratio (dimensionless)

V_s = volume of soil particles (cm^3)

The soil porosity or pore space is important because the pores are the means through which water enters the soil.

Since water is held in the pore space of soils, it is difficult to visualize moisture contents. It is therefore convenient to define soil moisture as either gravimetric moisture (θ_g) or volumetric moisture (θ_v) (usually expressed as a percentage). Gravimetric moisture is the water content of a particular soil on a weight basis, given as:

$$\theta_g = \frac{M_W}{M_{DS}} x\,100 \tag{3}$$

where:

M_W = mass of water (g)

M_{DS} = dry weight of soil (g)

The volumetric water content is defined as the volume of water per volume of moist soil. Gravimetric moisture is converted to volumetric moisture by multiplying by the bulk density. The bulk density (γ) is the ratio of oven dry weight of soil to total volume at the water content at which the measurement is made.

$$\theta_v = \theta_g \, x \, \gamma \tag{4}$$

where:

γ = bulk density (g/cm^3)

Now that a basis for calculating soil moisture has been established, it would be beneficial to categorize general soil-water terms. The most universal terms used to describe soil moisture can be divided into three classes: gravitational water, available water and unavailable water. Gravitational water is water which drains freely from the soil. Available water is described as the moisture which may be taken up from the soil by a plant. Unavailable water is defined as water held in the soil after the plant has permanently wilted.

Further terms used to describe moisture in soils include wilting point and field capacity. Wilting point refers to water held at 15 bars (approximately 225 lbs/in^2). Field capacity is the amount of water that soil can retain after gravity has caused water to drain away. After gravity drainage the moisture remaining in the soil is held by capillary tension. Capillary tension is affected by the particle size. In general, particle size is inversely proportional to capillary tension, i.e., as particle size increases, tension decreases and allows water to drain by gravity.

The moisture tension of soils, usually expressed as suction, is measured in terms of depth of liquid or force per unit area. Different soil types have different soil moisture tension relationships. The moisture retention curves shown in Figure 1 compare four soil classifications (sand, sandy loam, clay, and silt loam) to the Colbert fly ash used in performing the experiment. These four soils represent a variety of differences, such as structure, texture, and chemical properties. It would be helpful if a comparison could be distinguished between any fly ash and a particular soil classification. Then, if a numerical model was developed based on similar characteristics determining sensitive parameters would be easier. In order to examine the hydraulic properties of both the four soils and the Colbert fly ash, moisture retention curves were developed from existing data. These curves provided useful data and insight to hydraulic information such as residual moisture content, relative conductivity, capillary fringe, and the air entry value. For instance, calculations of relative conductivity were dependent on the residual water content. At the residual water content the relative hydraulic conductivity was zero; therefore, most capillary models required the retention characteristics curve to the point of residual water. Other parameters such as capillary fringe and the air entry value (a turning point) were important in

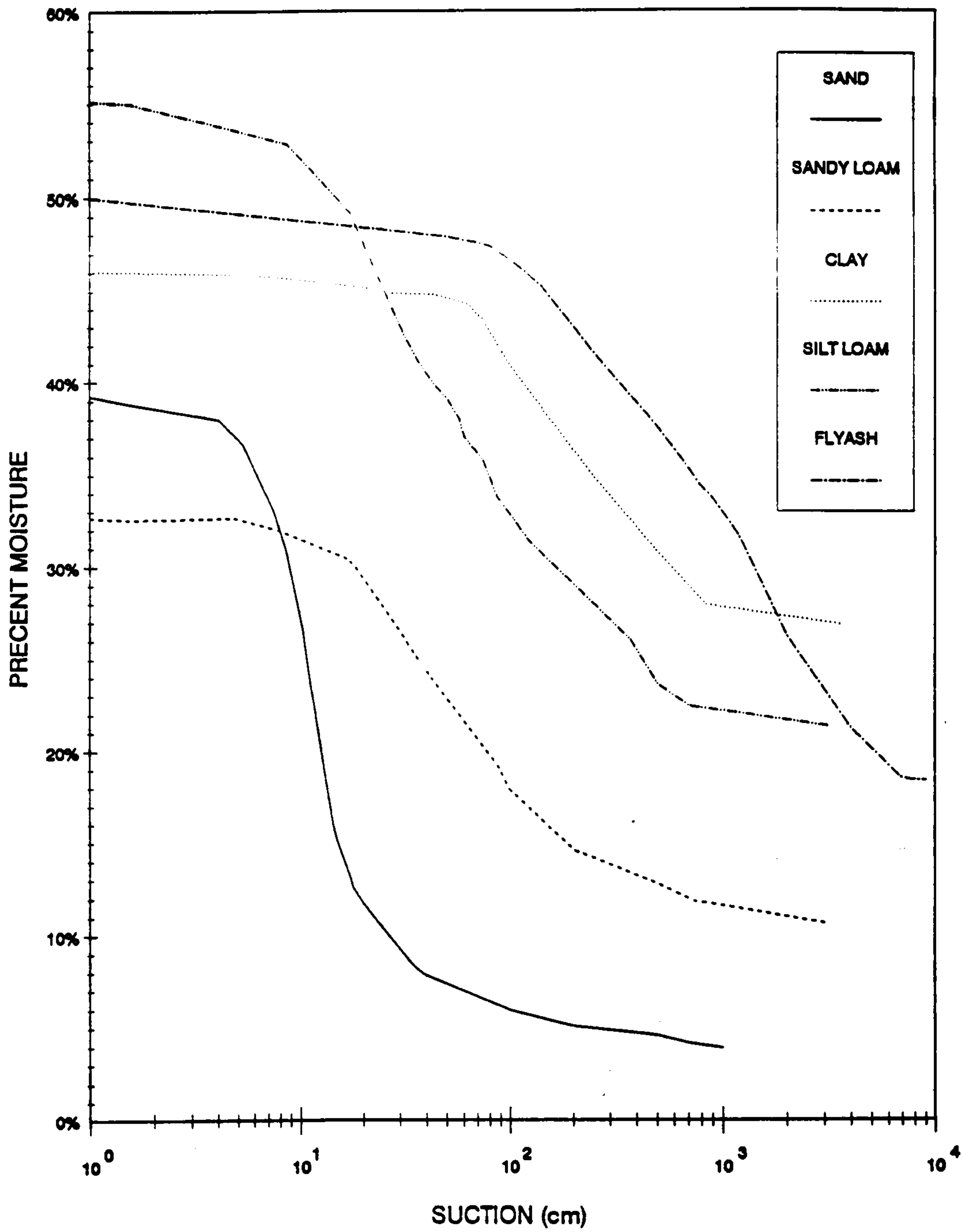

Figure 1. Moisture Retention Curves of Suction versus Percent Moisture of Four Soils of Different Texture Compared to a Colbert Fly Ash Moisture Retention Curve.

Soil Curves Adapted from R. L. Hausenbuiller, 1972, <u>Soil Science Principles and Praticies.</u>

determining decreases in hydraulic conductivity from the saturated conductivity. Figure 2 shows an idealized water retention characteristic curve with the capillary fringe area, air entry pressure, and residual water content identified.

Capillary forces and air entrainment also merit consideration in the analysis of soil moisture and its vertical movement. The height of upward capillary movement of moisture is a result of particle size. The analogy of capillary rise is often demonstrated with glass tubes placed in a dish of water. In order to incorporate soil particle sizes in the explanation, four tubes (two empty tubes of different diameter sizes and two tubes filled with different soil particle sizes) are placed in a dish of water. Figure 3 shows the relative upward movement by capillarity in the four tubes. The large diameter tube (a) and coarse-textured soil (b) show a smaller rise when compared to the small diameter tube (c) and fine-textured soil (d). Because the diameter size affects the height of water rise, it is recognized that the strength of the attraction between the water and the glass tube or soil particle is proportional to the radius. This concept is given as:

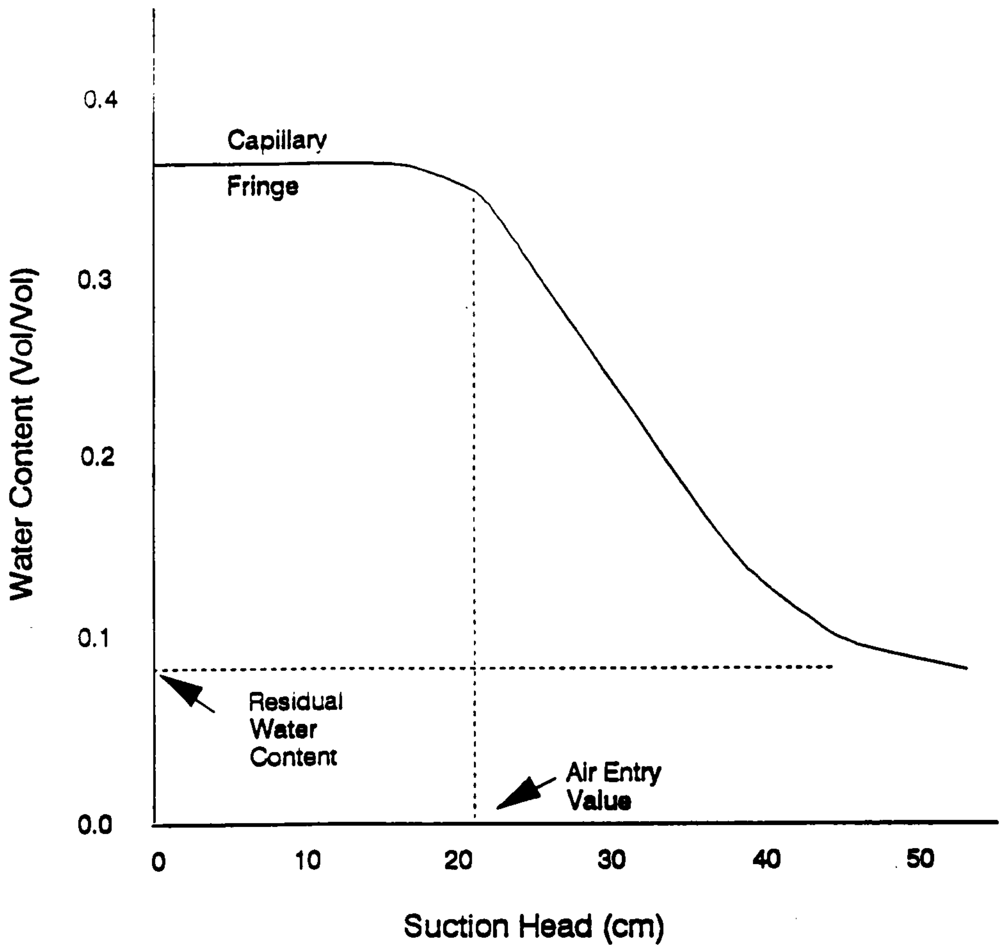

Figure 2. Idealized Water Retention Characteristic Curve Illustrating the Relationship Between Capillary Fringe Area, Air Entry Value and Residual Water Content in a Continuous Saturated-Unsaturated Soil System.

Curve Adapted from Bond etal., 1984, UNSAT1D Computer Code Manual: IBM Version, EPRI CS-3747.

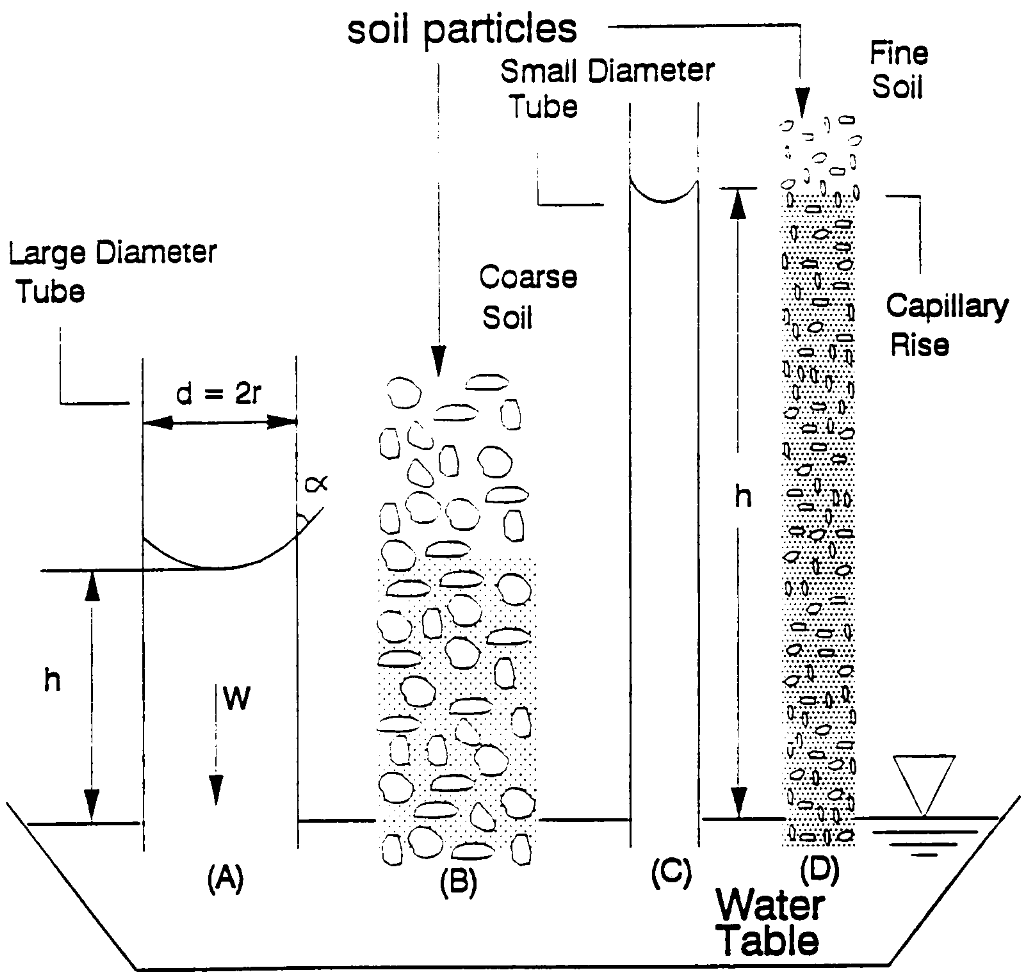

Figure 3. Relative Capillary Water Rise in a (A) Large Diameter Tube, (B) Coarse Soil, (C) Small Diameter Tube, and (D) Fine Soil.

$$h = \frac{2T\cos\alpha}{r\gamma_w} \qquad (8)$$

where:

h = height of rise in the capillary (cm)
T = surface tension of water (g/cm)
α = angle of contact of water and soil
γ_w = density of water (g/cm^3)
r = radius of capillary (cm)

Entrapped air is considered to affect the soil moisture characteristics by decreasing the conductive properties of the soil. During the water entry process, air is sometimes trapped below the wetting front. This trapped air is forced down into the soil, where it forms a pocket. Air pockets such as these prevent the complete saturation of soil and create small errors in soil-moisture curves.

2.3 Soil Water Potential

Gardner and Hsien (1955) describe soil water flow as "a process caused by a driving force resulting from a hydraulic gradient flowing in the direction of decreasing energy potential." The rate of flow is proportional to the potential gradient, and it is affected by the channels through which water passes. In an isothermal system, the driving force for transport of soil water is the gradient of potential energy.

The energy concept was first applied to soil water movement by Buckingham in 1907. In 1963, Aslying redefined this concept:

> "The total potential energy of soil water is defined as the amount of work liberated by moving a unit mass of soil water to a certain location in the soil in the form of pure free water at the same temperature, and to isothermally transfer this quantity to another reference level, where, it is defined as having a potential energy of zero."

The total potential energy (ψ_T) of soil water can be thought of as the sum of separate contributions of gravitational (ψ_g), pressure (ψ_p), and osmotic (ψ_o) potential, or

$$\Psi_T = \Psi_g + \Psi_p + \Psi_o \tag{5}$$

where:

ψ_T = total potential energy (cm)
ψ_g = gravitational potential (cm)
ψ_p = pressure potential (cm)
ψ_o = osmotic potential (cm)

Not all of the aforementioned energy potentials act the same, and their individual gradients are not always equally effective in causing flow. The total potential concept produces a unified measure by which the state of soil water can be evaluated at any time and any place within the soil-plant-atmosphere continuum. The quantity may be chosen as unit mass, weight, or volume (Hillel, 1971). These potentials are described as follows.

The gravitational potential is due to the earth's gravitational force. By selecting the soil surface as the datum and z as the depth below the surface, the gravitational potential will equal negative z. In other words, gravity causes pressure to vary with elevation. By using Bernoulli's equation as related to pressure, velocity, and elevation between two points of different elevation, a graphical illustration shown in Figure 4 defines gravitational potential or gravitational head z.

Pressure potential describes the total pressure head resulting from a force on a constrained volume of water. Because water is virtually incompressible, the force and containment results in an increase or decrease in internal pressure. In unsaturated soil, the pressure head is negative due to the forces of capillarity and short range adsorption forces between water molecules and the soil matrix. These forces are responsible for the retention of water in the soil. However, in the saturated zone below the phreatic surface, the attraction of the soil matrix is negligible, and hydrostatic pressure governs so that the values for ψ_p are positive.

Osmotic potential occurs as a result of solutes

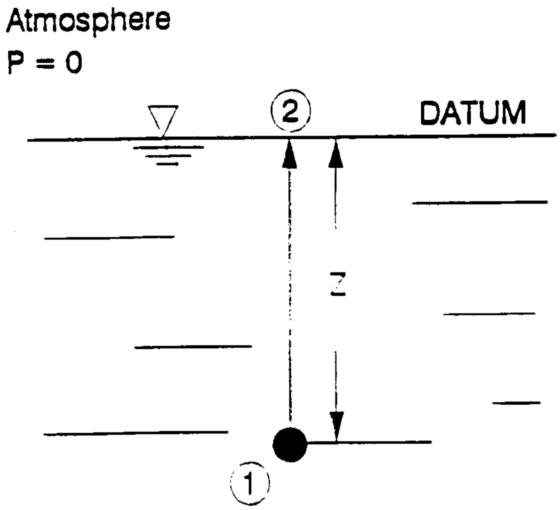

Bernoulli's Equation

$$P_1/\gamma + V_1^2/2g + Z_1 = P_2/\gamma + V_2^2/2g + Z_2 \qquad (1A)$$

where:

- P = pressure (N/m^2)
- γ = specific weight (N/m^3)
- Z = elevation (m)

Assuming that ↑ is positive and the velocity of point 1 and 2 are equal, the velocity heads ($V^2/2g$) cancel each other and equation 1A is reduced to the following:

$$P_1/\gamma + Z_1 = P_2/\gamma + Z_2 \qquad (1B)$$

Now considering point 2, located at the datum or surface where both P (atmospheric pressure) and Z (elevation) are zero then Equation 1B can be written as:

$$P_1/\gamma + Z_1 = 0 \quad \text{or} \quad P_1/\gamma = -Z_1 \qquad (1C)$$

Figure 4. Graphical Illustration and Derivation of Gravitational Head Using Bernoulli's Equation to Show the Relationship Between Elevation and Pressure.

present in the water. This pressure is generally proportional to the concentration of the solution and to itstemperature, according to the following equation:

$$\psi_o = kTC_s \tag{6}$$

where:

k = boltzmann constant (1.37×10^{-6} erg $^\circ$K)
T = temperature $^\circ$K
C_s = concentration of the solute

However, in soil water, solutes move freely with the water, and gradients due to osmotic potential are negligible (Hillel, 1971).

2.4 Hydraulic Conductivity and Diffusivity

The mathematical foundation of unsaturated soil water flow equations, whether analytical or numerical, requires knowledge of the soil media's hydraulic conductivity or diffusivity as a function of moisture content. For unsaturated soils, both hydraulic conductivity and diffusivity change with moisture content.

Hydraulic conductivity, K, is a measure of a porous media's ability to transmit water. This relationship of moisture content and hydraulic conductivity was presented by Richards in 1928 (Philip, 1972). When a soil is saturated, K is considered to be at the maximum value, and any decrease in moisture content results in a decrease in conductivity.

The variation of K with moisture content can be understood by considering the soil water flow path. As any soil dries, the first pores to drain are the largest ones, which are the most conductive. As pores empty, the length of the flow path increases. This hinders the soil's ability to move moisture both horizontally and vertically; therefore causes the hydraulic conductivity to decrease (Hillel, 1971).

In the analysis of unsaturated flow equations, rearranging the mathematical expressions into a form that utilizes diffusivity is sometimes more beneficial, because the variation of diffusivity is smaller than that of hydraulic conductivity. Diffusivity, D, is the ratio of the hydraulic conductivity to the specific water capacity. The specific water capacity term relates to the slope of a capacity curve at a particular water content ($d\theta/dh$), given as:

$$D = \frac{K}{C} \tag{7}$$

where:

D = diffusivity (cm_2/sec)
K = hydraulic conductivity (cm/sec)
C = specific water capacity $d\theta/dh$ (cm)

The diffusivity concept considers K and C to be both position and water-content dependent (Klute, 1972). This concept was originally suggested by Childs and Collis-George (1950), and represents a combination of Darcy's law with the equation of continuity for the conservation of matter

(Klute, 1952). The diffusivity concept in relation to the process of liquid water movement in soils is that of mass flow. Therefore, inconsistent results may be exhibited: (1) when suction versus moisture hysteresis is appreciable; (2) when the soil is layered; or (3) in the presence of a thermal gradient.

2.5 Hysteresis

Suction versus moisture hysteresis is an important phenomenon to consider when analyzing vertical and horizontal soil-moisture characteristics. Hysteresis is caused by a number of factors, the most important of which is the entrapment of air during wetting. Another factor is that as a soil dries, its colloids shrink. Upon rewetting, the pore configuration is not always the same. Figure 5, a suction versus moisture hysteresis curve, depicts this effect graphically. The curve shows that, given the same moisture content (gravimetric or volumetric moisture), suction heads from the initial drainage curve (IDC) vary from suction heads of the main wetting curve (MWC). The wetting curve for a given moisture content usually corresponds to a lower suction head, while the drying curve exhibits a higher head for the same moisture percentage. It

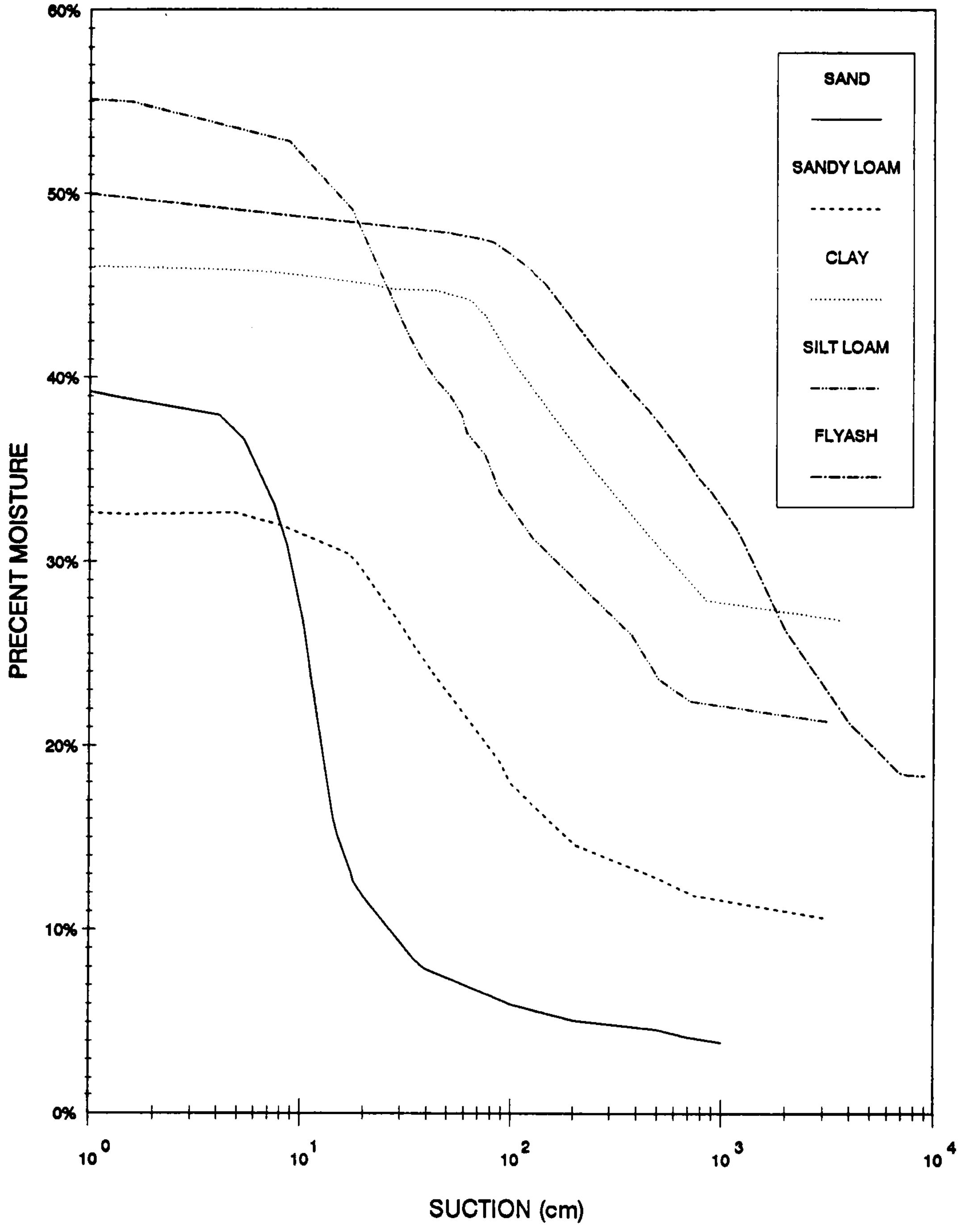

Figure 5. A Hypothetical Drying and Wetting Curve Illustrating the Relationship Between Moisture Content and Suction Head. The Hysteretic Loop Shows that the Same Moisture Content for the Wetting Curve and the Drying Curve Have Different Suction Heads.

is important to note that selecting wetting or drying curve values affect the modeling output.

Typically, the issue of suction versus moisture hysteresis is commonly neglected in the analysis of both horizontal and vertical water movement in the unsaturated zone. This oversight is attributed to the difficulty of collecting necessary data (Kaluvachchi and Parker, 1978). Ignoring hysteresis may induce error into the results. The amount of error depends on the extremes of the measured values. In most studies involving soil water movement, especially in practical applications, hysteresis effects are important and should not be neglected (Royer and Vachaud, 1975).

2.6 Unsaturated Flow Equations

The theory of unsaturated flow involves the mathematical relationship of various flux components and the appropriate driving forces. The derivation of unsaturated flow equations stem from Darcy's law which was originally formulated for saturated flow. In 1931, L. A. Richards modified Darcy's law to model unsaturated flow.

Henri Darcy (1856) discovered that velocity for 1-dimensional vertical flow of a saturated medium is proportional to the hydraulic gradient,or

$$q = -K \frac{dH}{dz} \tag{9}$$

where:

q = flux, volume of liquid moving through a unit cross-sectional area of soil per unit of time (cm/s)

K = hydraulic conductivity (cm/s)

dH/dz = total head (cm)

The negative sign denotes that flow moves in the direction of decreasing head.

For conditions where the medium is only partially saturated, Equation 9 was modified to account for changes in hydraulic conductivity as a function of moisture content.

$$q = -K(\theta) \frac{dH}{dz} \tag{10}$$

where:

$K(\theta)$ = hydraulic conductivity function (cm/s)

θ = volumetric moisture content (vol/vol)

The continuity equation for one-dimensional flow may be represented by:

$$\frac{d\theta}{dt} + \frac{dq}{dz} = 0 \tag{11}$$

where:

q = flux (cm/sec)

t = time (sec).

Equations 10 and 11 yields a differential equation of the water flow in the vertical direction, of the unsaturated soil, commonly referred to as the Richard's Equation, or:

$$\frac{d\theta}{dt} = \frac{d}{dz}\left[K(\theta)\frac{dh}{d\theta}\frac{d\theta}{dz}\right] - \frac{dK}{dz} \tag{12}$$

where:

θ	= moisture content (vol/vol)
z	= depth (cm)
K	= hydraulic conductivity (cm/sec)
t	= time (sec)
h	= capillary suction (cm)

As discussed in Section 2.3, using diffusivity (D) is often convenient to describe unsaturated flow. Representing D as $K(\theta)(dh/d\theta)$ in Equation 12 gives:

$$\frac{d\theta}{dt} = \frac{d}{dz}\left[\left(d(\theta)\frac{d\theta}{dz}\right) - \frac{dK}{dz}\right)\right] \tag{13}$$

This is another form of Richards Equation, based on diffusion-moisture relationships (Chow, et al., 1988), and either form may be used, depending on available data. A simplified approach to solving vertical soil-moisture movement is the Green and Ampt (1911) model of infiltration. The model assumes that the moisture profile may be approximated by a uniform saturated wetting zone separated from the dry initial condition defined by a sharp wetting front as shown in Figure 6. The Green and Ampt model is represented as:

$$i(t) = K_s\left[\frac{1-k_{Ri}+\theta(H_o+H_f)}{F(t)}\right] \tag{14}$$

where:

$i(t)$ = infiltration rate (cm/s)
K_s = hydraulic conductivity of the transmission zone (cm/s)
k_{Ri} = relative conductivity function value at the initial moisture content (cm/s)
H_o = pressure head at the entry surface (cm)
H_f = effective pressure head (cm)
θ = net gain in moisture (g/cm^3)
$F(t)$ = cumulative infiltration (g/cm^3)

2.7 Evaporation

Evaporation is an important part of the hydrologic cycle. This phenomenon involves the perpetual exchange of water between the atmosphere and the earth's surface. The term evaporation applies to both water surfaces and land surfaces. Three criteria must be met in order for evaporation to occur: an energy supply must be supplied, vapor must be removed, and water must be supplied at the surface where evaporation takes place (Hillel, 1971). The first two conditions are externally influenced by wind, velocity, humidity, net radiation (incoming solar and indirect radiation minus outgoing reflected and emitted radiation), and ambient temperature. The third condition is internal and is affected by the properties of the porous medium.

The majority of formulae or models used to predict evaporation and evapotranspiration can be divided into three

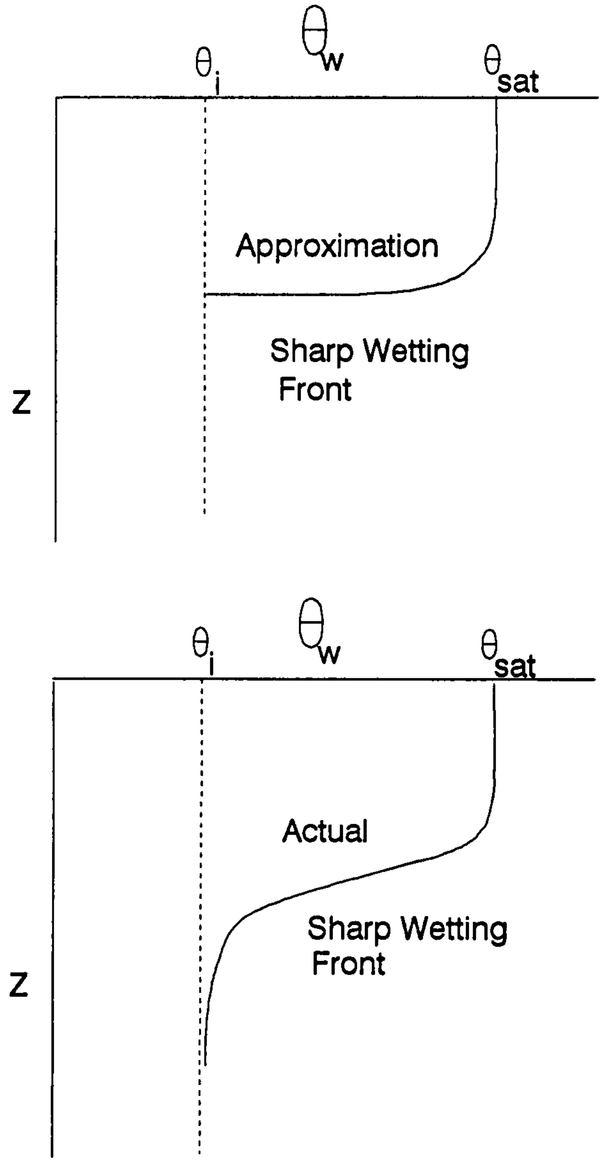

Figure 6. Graphical Illustration of an Approximated Wetting Front as Compared to an Actual Wetting Front used to Represent the Moisture Profile Assumed by the Green and Ampt Model of Infiltration.

groups:

- energy balance
- mass transfer
- water budget

The energy balance approach considers conservation of energy at the surface and requires heat for evaporation of water. Thus, if there is no change in water temperature, the net radiation or (heat supplied) is a measure of the latent heat of evaporation. The mass transfer method recognizes that moisture moves away from evaporating surfaces in response to the wind and the vapor pressure gradient between the evaporating surface and overlying conditions. The water budget analysis examines the hydrologic cycle and evaluates water movement based on the law of conservation of mass at the evaporating surface. In the simplest form, the water balance or storage is represented as water in minus water out. A schematic diagram showing the primary components of the water budget are shown in Figure 7. The water balance equation for a given controlled volume and finite time interval is:

$$P - E - R - D = \Delta S \tag{15}$$

This section has focused, up to this point, on free water surface evaporation. Since the previous sections (2.1 - 2.4) lay the ground work for soil-water movement, now it

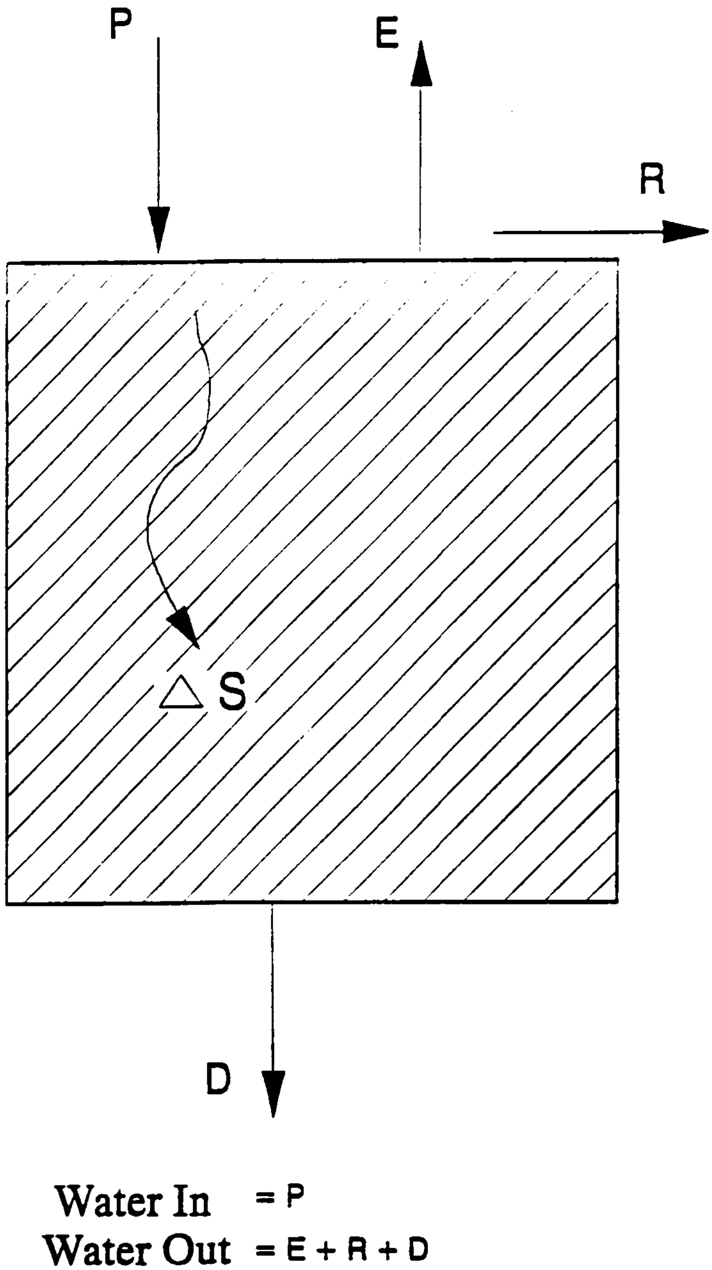

Figure 7. Schematic Diagram Illustrating the Components of a Water Budget for a Soil System.

becomes necessary to include a soil moisture function in order to analyze evaporation from a soil surface. Soil-moisture evaporation is often described as a two-stage process (Ritchie, 1972). The first stage is controlled by atmospheric conditions, while the second stage is limited by the soil's ability to transmit water.

First stage evaporation is usually characterized by a relatively high evaporation rate governed by atmospheric conditions. During this stage, the moisture in the soil is removed at a rate that gradually approaches, but never surpasses, the potential evaporation rate. The potential evaporation rate. The potential evaporation is defined as the water loss which occurs if there is at no time a deficiency of water in the soil (Viessman, 1977), or if there is an infinite supply of water at the surface. The external atmospheric conditions propagate the removal of moisture; then as water is removed from the surface, the soil gradually dries. This drying of the soil surface creates a hydraulic gradient causing moisture to move upward. During first stage evaporation, the soil transmits water to the surface to meet evaporative demands. When the soil can no longer transmit enough water to the surface to meet the evaporative demand, the evaporation rate is controlled by the hydraulic properties of the soil. At this point, second stage evaporation begins. The concept of two-staged evaporation has been used to develop models capable of analyzing evaporation of bare surfaces. However, it can be very difficult to distinguish when first stage evaporation ends and second stage evaporation begins.

Theoretically, evaporation losses from bare soil can be computed from decreases in the soil profile water content with time. By rearranging the Richards equation, (12), changes in water content are shown as:

$$\frac{d\theta}{dt} = \frac{d}{dz}\,[D(\theta)\ d\frac{\theta}{dz}] - \frac{d}{dz}\,[K(\theta)] \qquad (15)$$

This equation assumes 1-dimensional flow, isothermal conditions, a homogeneous soil profile and a uniform moisture content. However, Equation 15 is not easily solved because $D(\theta)$ and $K(\theta)$ are highly nonlinear, and because $D(\theta)$ is hysteresic. Assuming that gravity may be neglected (Childs, etal., 1950), the problem is simplified. Equation 16 reduces to:

$$\frac{d\theta}{dt} = \frac{d}{dz}\,[D(\theta)\frac{d\theta}{dz}] \qquad (16)$$

No exact solution to the equation exists, only approximations. Two methods used to reach an approximate solution are the linear solution obtained by a weighted-mean diffusivity calculated by Crank's method and a graphical technique obtained by iteration for the exponential type diffusivity. Both methods are equally effective and quite suitable for most soils (Britsaert, 1979b).

3.0 NUMERICAL MODELS

3.1 One-Dimensional Models

The evaporation models being evaluated in this study are:

- UNSAT1D
- Hydraulic Evaluation Landfill Performance Version 2 - HELP2
- Wetting Front Model

These models employ infiltration, redistribution after infiltration, evaporation, and drainage. As stated earlier, the objective of this thesis is to evaluate the evaporation process of each model in relation to the column study data.

3.1.1 UNSAT1D

UNSAT1D is a fully implicit, finite-difference code that simulates one-dimensional flow through unsaturated or partially saturated underground regions (Bond and Dawson, 1987). The unsaturated groundwater flow model simulates infiltration, vertical seepage, soil layering, evapotranspiration, and root growth characteristics. The modeling package consists of a computer code to make the unsaturated flow predictions, several support codes for the preparation of input data, and the evaluation and display of model results.

The modeling package consists of 14 subroutines divided into 3 groups. The first group is composed of pre-processing programs designed to assist the user in the preparation of necessary input data and parameters. Next are solution subroutines used to simulate one-dimensional flow in partially saturated porous media. Finally, the post-processing routines are designed to assist the user in the interpretation of results.

Soil data requirements of the model include: (1) depth of soil layer; (2) lower boundary condition; (3) initial moisture content; (4) porosity, and (5) soil hydraulic properties. The soil-water retention relationship is one of the required soil hydraulic properties. Meteorological data and vegetation information needed for input to the model include hourly distribution of precipitation, potential evaporation values, and plant growth characteristics. Other input requirements include time step control parameters, spatial resolution used in defining the location of grid points, and averaging procedure for representing the conductivity between nodal points.

The material being analyzed is divided into a grid network. There are no fixed rules for identifying an appropriate grid spacing without trial and error. The model uses a time step based on a user specified convergence criteria. The parameters used to control the adaptive time step are minimum time step, maximum time step, step size increase factor, parameters used for checking convergence, and a tolerance parameter. The model follows a systematic order of routines in the analysis:

- HAVERFT
- UNSATINP
- DATAIN
- UNSAT1D

HAVERFT is used to curve-fit the hydraulic data. Each moisture content is associated with a suction head. Once a satisfactory curve is developed, the data are written into an output file. The output file developed by HAVERFT is used as input for UNSATINP. UNSATINP performs basic calculations and writes a binary output file. This output file is used as input for DATAIN. Execution of DATAIN is necessary to format the input file for UNSAT1D from UNSATINP. Once all the preliminary codes are finished, UNSAT1D estimates the water budget based on the input. For further information refer to Gupta, et al., 1978.

UNSAT1D simulates the removal of soil moisture as two independent processes, the first being transpiration by vegetation, and the second is soil surface evaporation. Transpiration from vegetation and evaporation from soils are affected by the same climatological variables, and both involve similar basic processes. However, soils and crops constitute two different pathways as water moves to the evaporating surface.

In the soils, the moisture flows through the water-filled pores to the surface. The actual evaporation is determined by either the external atmospheric evaporative demand or the rate of water supply to the soil surface, the smaller being the limiting factor. The evaporation from vegetation occurs from the stoma of leaves. The major part of the exchange of water vapor and carbon dioxide to the atmosphere occurs through the leaves.

To compute transpiration, the model requires a leaf-area index value and potential evapotranspiration. This value is the ratio of leaf to ground area and is influenced by plant population, variety, row spacing, fertilizer, and water applied. Equation 18 is used to calculate transpiration from plants:

$$PT = PET(-.21 + .70(LAI)^{.5}) \tag{17}$$

where:

PT = total potential
LAI = leaf-area index (dimensionless)
PET = potential evapotranspiration (cm/day)

The constant used in Equation 17 was derived from experimental data (Ritchie and Burnett, 1971).

The daily potential evapotranspiration used in the equation, is either measured or calculated by one of the following methods:

- Blaney-Criddle
- Radiation
- Modified Penman
- Evaporation Pan Method

Since this evaporation study involve a bare surface, the transpiration term was assumed zero and the potential evaporation was measured.

The calculation of evaporation for the model was based on an empirical formula developed from a field lysimeter study by Beese, et al. (1977). The study was carried out for a period of 218 days using an undisturbed fallow loessial soil. The results from the study are graphically presented in Figure 8, and the empirical formula derived from the study is presented as:

$$\frac{E}{E_o} = -0.5767\ Log(h) + 1.78 \tag{18}$$

where:

E = predicted surface evaporation (cm)
E_o = potential evaporation (cm)
h = pressure head (cm)

3.1.2 HELP2

The HELP2 model was developed by the U.S. Army Corps of Engineers for the Environmental Protection Agency (EPA). Updated in 1989, the HELP2 model is a quasi two-dimensional deterministic computer code that generates water budgets for a landfill by performing a daily sequential simulation of water movement into, through, and out of a landfill (Shroeder, 1988). It does not account for lateral inflow or surface run-on and is limited in application for up to 20

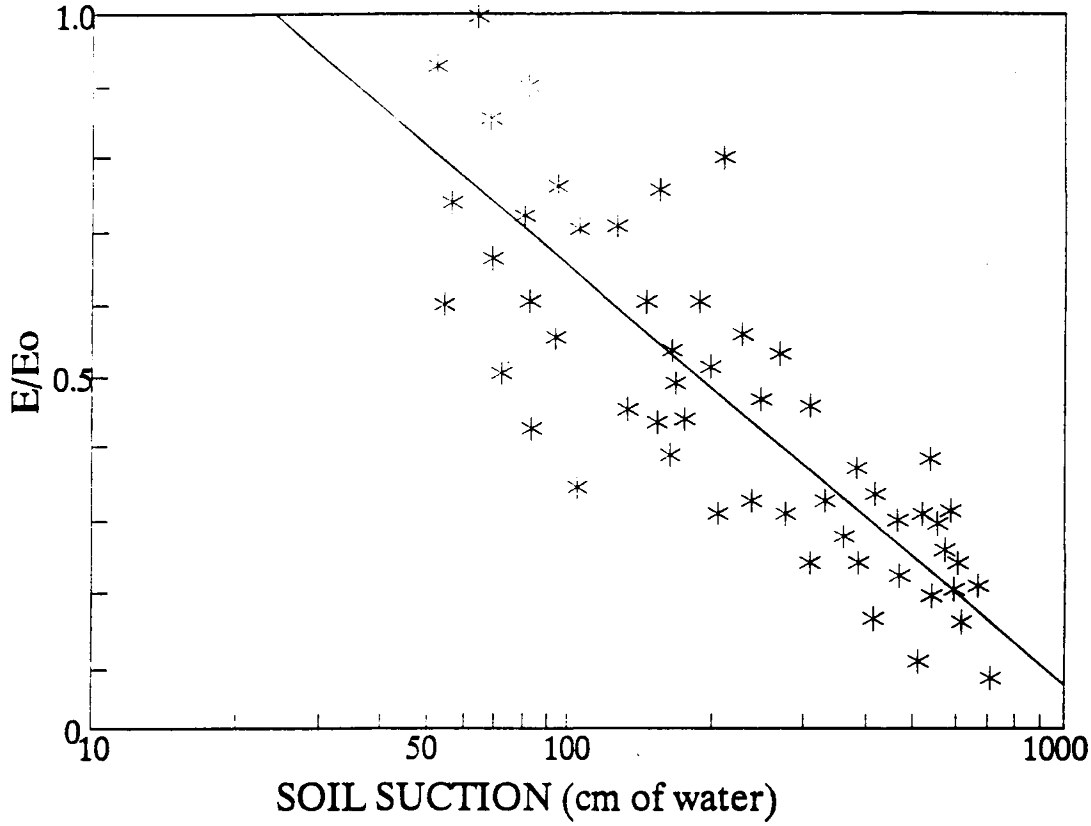

Figure 8. Ratio of Actual to Potential Evaporation versus Soil Suction Used in Developing the Empirical Equation for the Evaporation Routine in the UNSAT1D Code.

Curve Adapted from Beese, F., R.R. Van Der Ploeg and W. Richter, 1977, "Test of a Soil Water Model Under Field Conditions," <u>Soil Sci. Soc. of America Journal.</u>

years, based on statistical default data.

HELP2 offers a simpler alternative for water budget estimates. Requirements of the HELP2 model include soil, climate, and design specifications. The model contains five years of default data for 18 different soil types and climatological data for 102 cities in the United States to aid the user if no data are currently available. The soil input requirements include:

- porosity
- saturated hydraulic conductivity
- field capacity
- wilting point
- initial moisture content

The climatological input parameters include:

- daily precipitation
- daily solar radiation
- mean daily
- average monthly temperatures

Design input data necessary are thickness, type and number of layers.

The primary routines used to calculate the water budget are: (1) unsaturated hydraulic conductivity, (2) runoff, (3) unsaturated flow, (4) potential evaporation, and (5) evaporation. The individual Soil Conservation Service (SCS) components computed by the model include:

- infiltration
- SCS curve number
- evapotranspiration
- soil moisture storage
- vertical
- lateral flow

Runoff is calculated based on the SCS curve number, and infiltration is computed by subtracting the daily runoff from the net rainfall in inches. Evapotranspiration potential is estimated using the modified Penman method; storage is simulated by the water balance equation; and vertical flow is based on Darcy's law.

HELP2 estimates the unsaturated hydraulic conductivity by using a two-step process. The first step involves calculation of the pore-size distribution index using the Brooks-Corey equation (Brooks and Corey, 1964) to relate soil water content to capillary pressure by:

$$\left(\frac{Yb}{Y}\right)^{T} = \frac{(WC-WCr)}{(WCs-WCr)} \qquad (19)$$

where:

Yb = bubbling pressure (cm H_2O suction)
Y = capillary pressure (cm H_2O suction)
T = pore-size distribution index
WC = volumetric moisture content (vol/vol)
WCr = residual moisture content (vol/vol)
WCs = saturated moisture content or porosity (vol/vol)

The second step uses the pore-size distribution index and the power function of Campbell (1974) to calculate unsaturated hydraulic conductivity.

$$K(\theta) = Ks\left[\frac{(WC-WCr)}{(WCs-WCr)}\right]^{[3+(\frac{2}{T})]} \qquad (20)$$

where:

K(θ) = unsaturated hydraulic conductivity
Ks = saturated hydraulic conductivity

Additional equations used by the model to perform the unsaturated hydraulic conductivity calculation include:

$$WCr = .014+.253(WP) \tag{21}$$

$$T = -0.262\ln\left(\frac{(WP-WCr)}{(FC-WCr)}\right) \tag{22}$$

where:
WP = wilting point
FC = field capacity

Equation 21 defines the relationship between the wilting point and residual moisture content, while Equation 22 calculates the pore-size distribution coefficient use in the Brooks-Corey equation.

HELP2 simulates the rainfall-runoff extraction process by using the SCS curve number method (USDA, 1972). The technique assumes that for a storm event, the direct runoff (Q), in inches, is less than or equal to the depth of precipitation, (P), in inches. For a given rainfall event, runoff only occurs when the precipitation rate is greater than the infiltration rate and the initial demands of interception, infiltration, and surface storage have been satisfied. The sum of infiltration, interception, and surface storage is defined as the initial abstraction (I_a). The maximum amount of water that is retained at the surface before runoff begins represents the potential maximum retention (S). The empirical relationship between initial abstraction and potential maximum retention is:

$$Ia = 0.2S \tag{23}$$

where:
Ia = initial abstraction (in.)
S = potential maximum retention (in.)

Plotting runoff as a function of rainfall yields a curve that becomes asymptotic to a straight line with a 45° slope at high rainfall, as shown in Figure 9 (USDA, 1972). Equation 23 is based on data from a small watershed (less than one square mile in size) and large storms. Assuming no initial abstractions or lag between the times when runoff and rainfall starts, the equation of the straight line portion of the runoff curve, is:

$$Q = P-S \tag{24}$$

Now expressing the potential runoff as

$$P-Ia \tag{25}$$

and setting the ratios of actual quantities to potential

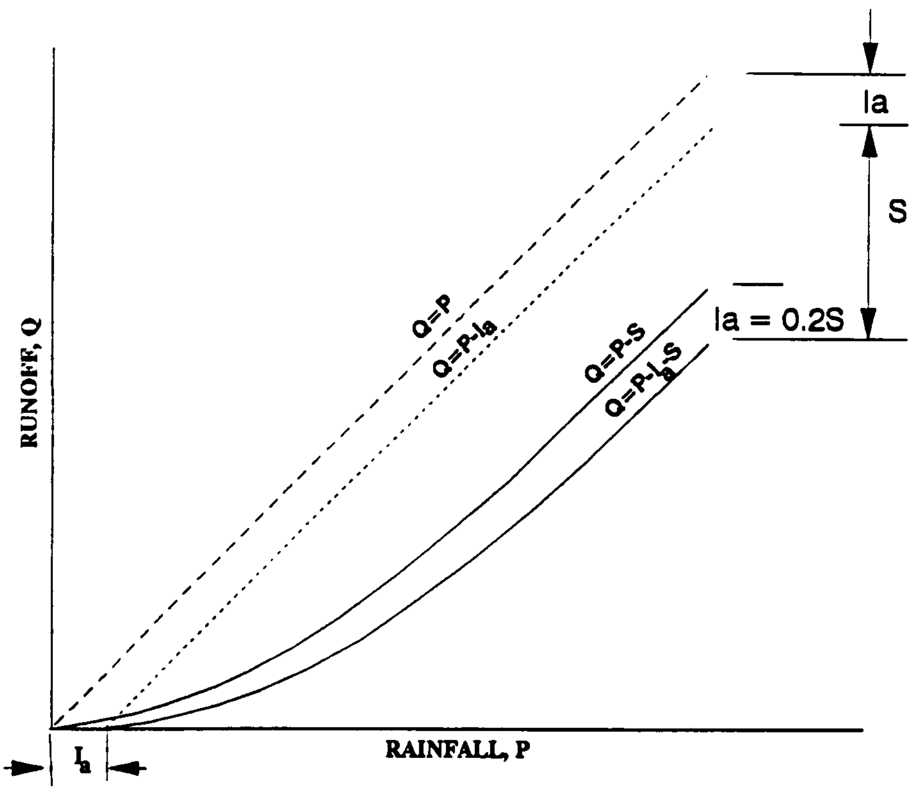

Figure 9. Graphical Relationship Between Runoff, Precipitation, and Retention Base on the SCS Curve Number Method.

quantities equal to each other yields

$$\frac{F}{S} = \frac{Q}{P} \tag{26}$$

where:

F = actual retention after runoff starts (in.), calculated as (P - Q).

Substituting F and solving for Q defines an expression for runoff as:

$$Q = \frac{(P - 0.2S)^2}{(P + 0.8S)} \tag{27}$$

where:

Q = actual runoff (in)
P = precipitation (in)

The curve number and S are related by

$$S = \frac{1000}{CN} - 10 \tag{28}$$

where:

CN = SCS curve number (0 - 100)

The calculation performed by the HELP2 model is based on antecedent moisture condition II, which represents an average soil moisture condition. If the value for the curve number for condition II is unknown, the HELP2 program will calculate it, based on:

$$CN(II) = Co + C1(MIR) + C2(MIR) \tag{29}$$

where:

CN(II) = curve number for condition II
Co,C1,C2 = coefficients that depend of the ground cover
MIR = minimum infiltration rate (inches/hour).

The HELP2 program uses the input curve number (condition II) in a fourth-order polynomial equation, (Equation 30), to directly calculate the curve number for condition I. The HELP2 program then uses Equation 31 to calculate the maximum retention parameter for condition I, which is referred to as "Smax." For each rainstorm, the value of the retention parameter changes according to Equation 31, which relates the antecedent soil moisture in the soil to the retention parameter used to calculate runoff in Equation 27.

$$CN(I) = 3.75x10^{-1}*CN(II)+2.757x10^{-3}*CN(II)^{2}-1.639x10^{-5} *CN(II)^{3}+5.143xE\text{-}7*CN(II)^{4} \tag{30}$$

$$S = \frac{Smax*(1-(\theta-WP)}{(\rho-WP)} \tag{31}$$

where:

CN(I) = curve number for a dry soil
Smax = maximum retention parameter for a dry soil
θ = average moisture content
WP = moisture content at wilting point
ρ = porosity

For vertical flow through waste layers, the HELP2 model ignores pressure potentials caused by capillary forces. Thus, vertical flow is characterized by:

$$q = K(\theta) \tag{32}$$

where:

$K(\theta)$ = unsaturated hydraulic conductivity function

The rate of evapotranspiration from a landfill is a function of the:

- potential evaporation rate
- surface wetness
- vegetative growth
- soil moisture conditions
- hydraulic properties of the soil

The condition of most interest for this study is the evaporation routine for bare soil. The HELP2 code first exerts the evaporative demand on available surface moisture that may be ponded or stored as snow on top of the landfill. After the surface moisture has evaporated, HELP2 evaporates moisture from a designated evaporation depth at a rate controlled by the evaporative demand (stage I evaporation) or at the rate controlled by the soil's hydraulic properties (stage II evaporation).

The HELP2 program uses Equation 33 to calculate the upper limit for cumulative evaporation occurring during stage II. Stage I evaporation occurs when the cumulative evaporation minus the cumulative infiltration is less than U (the upper limit of stage I evaporation).

$$U = \frac{[9(\alpha-3)*0.42]}{25.4} \tag{33}$$

where:

U = upper limit of stage I of evaporation, (inches)
α = evaporation coefficient, (mm/day$^{0.5}$)

When the difference between the cumulative evaporation and infiltration is greater than U, stage II evaporation occurs. Stage II is calculated by HELP2 using:

$$ES_{2i} = \frac{\alpha[0.5t_i-(t_i-1)^{0.5}}{25.4} \tag{34}$$

where:

ES_{2i} = stage II soil evaporation for day i, inches
t_i = days since stage I evaporation ended

The HELP2 model calculates the evaporation coefficient in Equations 33 and 34 based on empirical equations in Table 1. These coefficients are related to the unsaturated hydraulic conductivity of soils at -0.1 bar derived from experimental results of four soils (Ritchie, 1972) as shown in Figure 10. Evaporation coefficients (α) for four soils were determined experimentally from cumulative evaporation data during a single drying cycle. The data of each soil was plotted as a function of $t^{1/2}$, and the slope of the straight line represents the evaporation coefficient. Upper and lower limits are placed on the values of the evaporation coefficient to avoid exceeding the range of the experimental data.

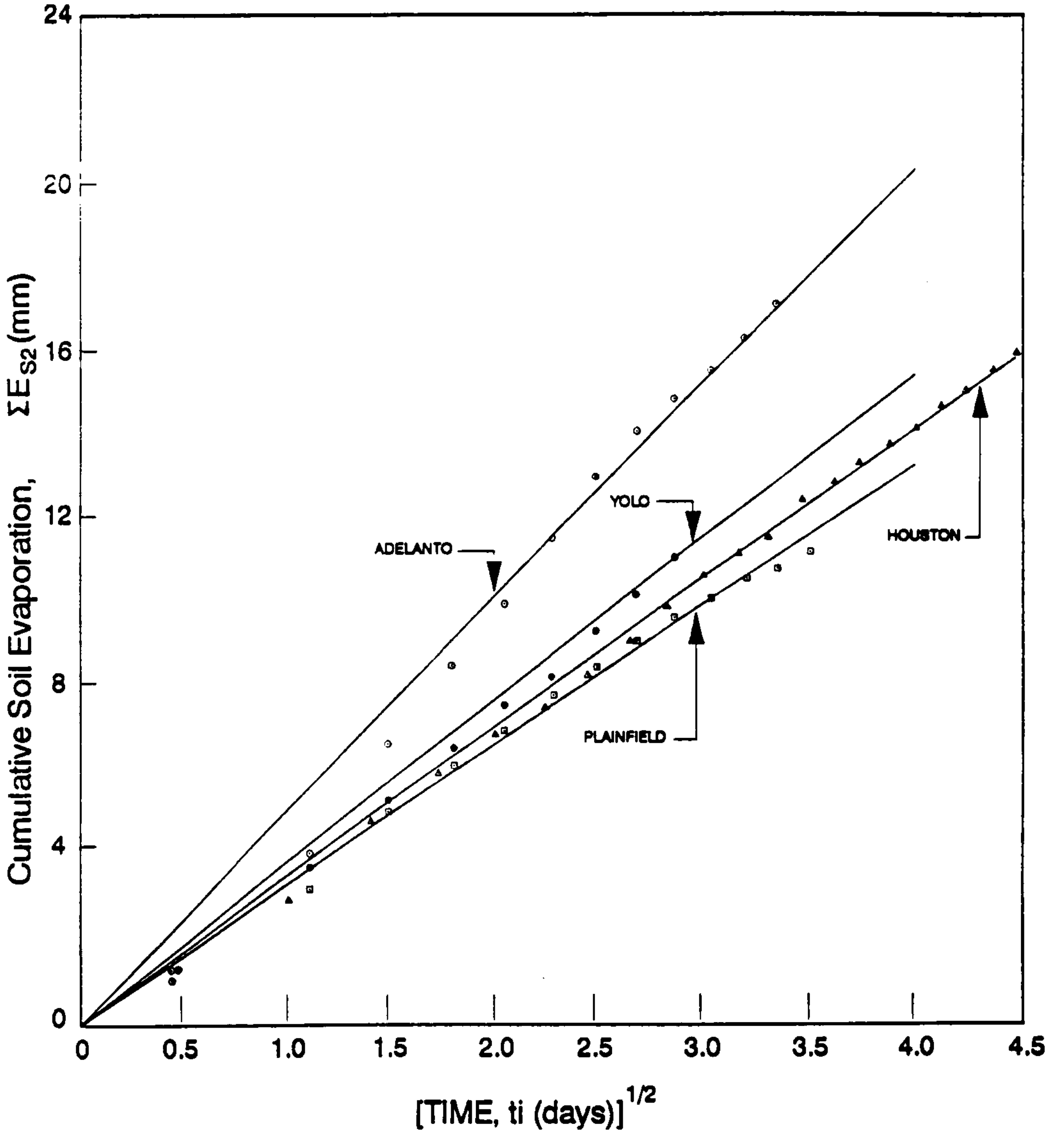

Figure 10. Experimental Results of Cumulative Soil Evaporation as Related to the Square Root of Time for Four Soils Derived from Field Study used in the HELP2 Evaporation Routine, (Ritchie, 1972).

Table 1.0 Evaporation Coefficients Derived from an Experimental Study Performed by Ritchie

Experimental Evaporation Coefficients, Alpha	
Evaporation Coefficient (α) mm/day$^{1/2}$	K (-0.1 bar) cm/day
3.3	K < 0.05
2.44 + 17.19(K)	.05 < K < 0.15
5.1	K > 0.15

The HELP2 model prevents evaporation from occurring if: (1) the temperature is below 32° F, and/or (2) a sufficient amount of water is unavailable in the designated evaporation zone. The evaporation zone depth is entered by the user and designates the depth from which water can be removed by evaporation. For instance, HELP2 recommends an evaporation zone depth of nine inches for bare soil in the geographic vicinity of Knoxville, Tennessee, however, the evaporation zone depth may in Tennessee vary from 3 to 9 inches.

The model calculates potential evaporation based on the modified Penman method used in the U.S. Department of Chemical Runoff and Erosion from Agricultural Management Systems (CREAM) Program (Knisel, 1980). The modified Penman method used in the HELP2 model for computing potential evaporation in inches of water was originally developed by Ritchie (1972). Equations used to generate potential evaporation values are given below.

$$PE = \frac{1.28 A_i H_i}{[(A_i + G) 25.4]} \tag{35}$$

$$A_i = \frac{5304\ e^{(21.255 - 5304/TK_i)}}{TK_i^2} \tag{36}$$

$$H_i = \frac{(1-L)\ R_i}{58.3} \tag{37}$$

where:

- PE = potential evapotranspiration (inches)
- A_i = slope of the saturation vapor pressure curve
- H_i = net solar radiation (langleys)
- G = psychometric constant, assumed to equal 0.68 (mb/°K)
- TK_i = mean temperature in degrees Kelvin on day i
- L = albedo for solar radiation, assumed to remain constant at 0.23
- R_i = solar radiation on day i (langleys)

The term for the slope of the saturation vapor pressure curve A_i is dependent on the mean air temperature on any given day. The albedo, L, is the ratio of the global short-wave reflected radiative flux and the flux of the corresponding incident radiation (Brutsaert, 1982).

3.1.3 Wetting Front Model

The Wetting Front (WF) Model is a one-dimensional, transient flow model developed to predict water budgets for bare soil surfaces. The model simulates the moisture profile of a soil by a series of blocks, each of which has a uniform soil moisture content. The blocks, called wetting fronts, are separated by abrupt changes in soil moisture. A new block is introduced at the surface at the beginning of a precipitation event. At the end of a precipitation event, the block continues downward in the profile, but the simulated rectangular shape elongates as the average soil moisture decreases, due to redistribution. The wetting fronts are "averaged out" when the blocks are merged. This happens when the moisture content at the wetting front, θ, or the distance between fronts, becomes sufficiently small. The model includes a negative storage term called the evaporation deficit, E*, which increases during inter-storm periods as the soil dries. In the model, E* also has a specific physical meaning, and it can be used to depict the gradual increase in θ with z, as shown in Figure 11.

The model requires, daily potential evaporation, hourly rainfall rates, soil hydraulic properties, and specific model parameters as input. Campbell's (1974) relationships for the soil hydraulic properties with the modifications proposed by Clapp and Hornberger (1976) are used. Some of the parameters required by the model include criteria for determining when wetting fronts should be merged and convergence criteria for allowing the time step to be changed as necessary to maintain acceptable results. As first described by Clapp (1982), the WF model has been

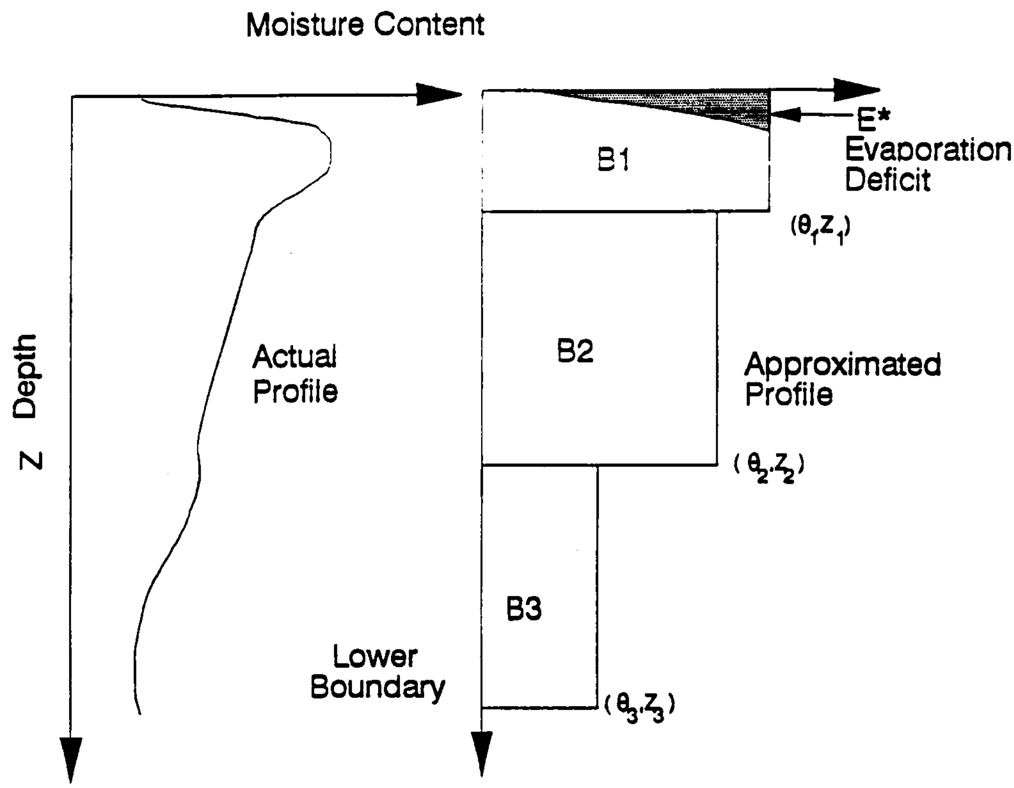

Figure 11. A Wetting Front Model Simulated Block Moisture Profile Derived from an Actual Moisture Profile.

modified to model flow in layered soils (Clapp, et al., 1983). The computational efficiency of the model relative to rigorous solutions by finite difference makes it an attractive tool. Clapp (1982) reported that for test simulation, the WF model required as little as three % of the computer CPU time required by an otherwise efficient, finite difference model. Markar and Mein (1987) reported similar efficiencies.

For rainfall infiltration, the model uses the Green and Ampt (1911) equation. To solve the Green and Ampt equation, the model calculates a wetting front suction, Ψf, according to Neuman (1976). Using the WF model and the appropriate notation, the infiltration rate (dI/dt) in cm/sec, is given as:

$$\frac{dI}{dt} = K_s \frac{\Psi f}{\Delta z_1} + Ks \tag{38}$$

where:

K_s = hydraulic conductivity at saturation (cm/sec)
Δz_1 = the depth to the wetting front (cm)

Before infiltration, the wetting front at $\Delta z1$ continues to move downward, following a relationship similar to Equation 38 except that unsaturated hydraulic conductivity replacing Ks and Ψf is diminished.

The treatment of evaporation in the WF model is described by what soil physicists refer to as evaporability. Evaporability, depicted as the soil-limited phase of evaporation, is estimated using the following expression:

$$\frac{dE}{dt} = \left(\frac{A}{2}\right) t^{-\frac{1}{2}} \tag{39}$$

where:

dE/dt = evaporation rate (cm/hr)
A = desorptivity

The desorption parameter A is an approximation of the weighted mean diffusivity for the desorption process. This approximation process given below was developed by Crank (1956).

$$A = \left(\frac{1.85}{(\theta_1-\theta_a)}\right)^{1.85} \int D(\theta_1-\theta_a)^{.85}\, d\theta \tag{40}$$

where:

A = weighted mean diffusivity
$\theta 1$ = initial volumetric profile wetness
θa = final volumetric wetness

The specification of any soil moisture value is problematic because of the continuous redistribution of θ (Clapp, 1982). Gardner, et al. (1970), showed that the rate of redistribution strongly affects dE/dt. Also, decreases in the rate beyond that reflected in the square root of time relationship prevail after rainfall or surface irrigation. Equation 39 can be integrated and reformulated as:

$$\frac{dE}{dt} = \frac{A^2}{(2E*)} \tag{41}$$

where E is the cumulative evaporation. In the WF model, E is replaced by the evaporation deficit E*, which is an approximated value and a function of evaporation and redistribution. However, for small infiltration, the deficit is overestimated. To overcome this problem, when infiltration is small (< 6mm), E* is evaluated as the difference between the cumulative evaporation and infiltration.

The fundamental premise of the WF model is that the field-water cycle may be described using Darcy's Law and the continuity equation. In the field cycle, evaporation is viewed as a two-stage process: initially, the surface flux is determined by the imposed meteorological rate, but later the soil properties near the surface limit that flux rate. For evaporation, the imposed rate (potential evaporation) is estimated from measurable, meteorological variables, in spite of the fact that those variables are coupled to the present state of the soil water beneath the surface (Clapp, 1982).

4.0 FLY ASH CHARACTERISTICS

4.1 Material Testing

The hydraulic and physical properties of the Colbert and Kingston fly ash were analyzed by Daniel B. Stephens & Associates, Inc. (1989). Ash samples used to determine the hydraulic parameters were collected directly from storage bins at the Colbert and Kingston Fossil Plant. The results from Stephens laboratory were used as input for each model.

4.2 Physical Properties

With respect to particle size (Figure 12), the Colbert and Kingston fly ash were categorized using the United States Department of Agriculture (USDA) classification system as silt sized soil particles. Approximately 85.1% by weight of both materials were within the silt-size range (0.002 to 0.05 mm), 11.5% were sand size (greater than .05 mm), and 3.37% were clay size (less than 0.002 mm). Figure 12 shows that the Kingston fly ash was somewhat smaller than the Colbert ash. The texture of the ash was very similar to loamy soils, while color is light gray but darker when wet. The average specific gravities of solid fly ash particles were estimated to be 2.23 for Colbert and 2.5 for Kingston. Bulk density of the materials was determined using procedures outlined under ASTM standard D698-78. These results showed Colbert and Kingston fly ash samples had dry bulk densities of 1.2 and 1.3 g/cc and

Sample No.	d_{10} (mm)	d_{50} (mm)	d_{60} (mm)	C_u	C_u
Colbert # 1	0.0052	0.020	0.025	4.81	1.11
Kingston # 1	0.0030	0.010	0.012	4.00	1.32

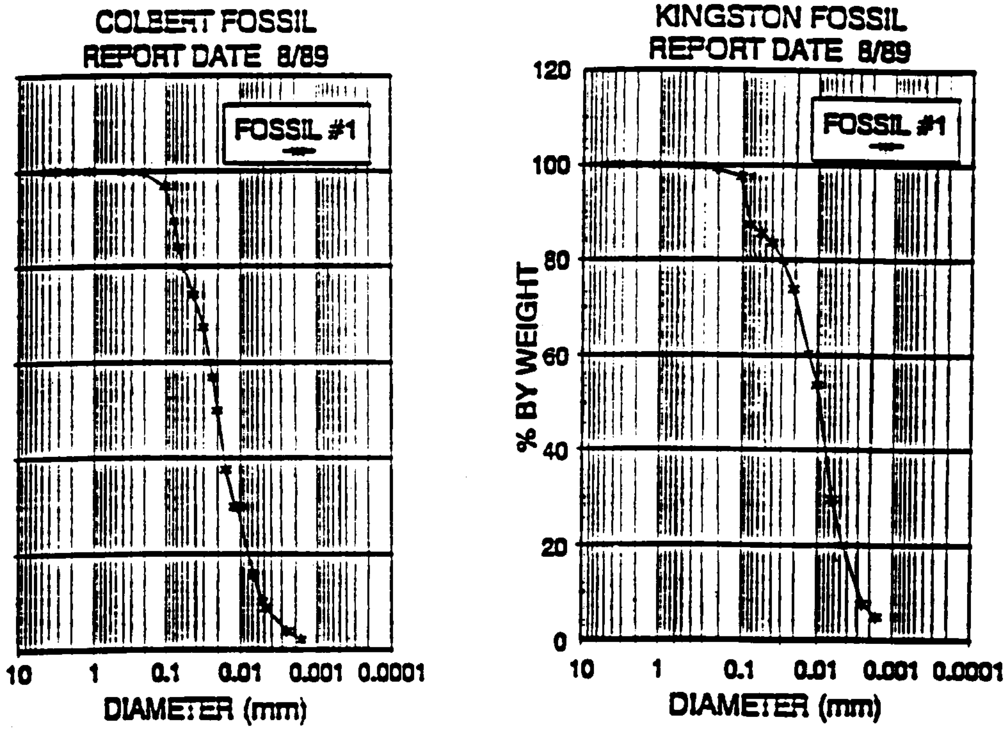

Figure 12. Particle Size Analysis for Colbert and Kingston Fly Ash Determined by Stephens Laboratory.

porosity values corresponding to densities of 0.4647 and 0.4605, respectively.

4.3 Hydraulic Properties

Saturated hydraulic conductivity (K_s) values were determined by the falling head at Stephens laboratory, (D. B. Stephens & Assoc., 1989). K_s values obtained from the laboratory procedure were 1.18E-04 (cm/s) for Colbert and 2.00E-05 (cm/s) for Kingston. Moisture retention data used by the models were determined using the hanging column and pressure plate procedures (D. B. Stephens & Assoc., 1989). These data included both the initial drainage curve and the main wetting curve; however, due to the conditions of the experiment (drying), only the data from the initial drainage curves were used.

5.0 Meteorological Data Base

5.1 Experimental Meteorological Data Base

In order to effectively model the evaporation of fly ash, a good meteorological data base is needed. A data base was created by performing a column evaporation study. The evaporation study was performed in-doors at the Norris Engineering Laboratory on Colbert and Kingston fly ash for a time period of 20 days.

The meteorological data collected during the study included relative humidity, temperature, wind speed and solar radiation. The data base provided the necessary input parameters for the water budget models and was also used to determine the atmospheric evaporativity. In order to determine the success or failure of collecting the meteorological data, intermediate measurements were collected during both experiments (approximately 3 times for each experiment) to provide a comparison or spot check of data measurements.

Since the monitoring equipment used in the study only checked temporal differences of wind speed, solar radiation, and temperature (i.e., constant over time), intermediate measurements were taken to check spatial differences of the same parameters (i.e., constant over different cylinders). Measurements of solar radiation, wind speed, and temperature were taken manually at the surface of each cylinder using a net radiometer, a portable wind speed sensor, and a thermocouple. The solar radiation and temperature measurements did not vary significantly; however, the cylinders positioned in the middle were somewhat higher (3-5 w/m^2 for solar radiation and 3°F in temperature). The difference in wind speed between for the Colbert fly ash columns and the Kingston fly ash columns (closest to the fan) was expected because of the position of the cylinders, with respect to the fans and the air circulation of the room. These measurements indicated an increase in wind speed of about .1 to .5 mph for the Colbert fly ash cylinders. Because of the spatial variability, the comparison between the actual evaporation result of the experiment and the modeled result (based on input data from the experiment), will focus on individual cylinders with similar climatological data.

The equipment used to collect the meteorological data included:

- humidity and temperature transmitter
- wind speed sensor
- net radiometer

Figures 13 and 14 show the meteorological data base collected for both 20 day experiments.

5.2 Meteorological Parameters

The relative humidity of the building which housed the experiment was not controlled. However, measurements indicated it ranged from 50 to 70% for both experiments.

The decrease in relative humidity at the end of experiment 1, (Figure 13), was due to an unnoticed change in the instrumentation position. During the course of the experiment, intermediate meteorological measurements, were taken, as previously mentioned. This backup data set for comparison was measured with additional portable equipment. In order to perform the measurements, the experiment instrumentation had to be moved from its original position for approximately two hours. Once the additional data was collected, the experiment instrumentation was put back in the original location and the experiment was brought back on line. Unfortunately, during the last measurement, the instrument used to measure relative humidity was over looked and the measurements taken during the time period of day 14 to day 20 for the first experiment were not representative of the actual conditions experienced by the ash. It was concluded that the relative humidity at the experiment site was different than that of the building. This measurement variation was omitted in the analysis of the data but was included in the graph and explained as previously stated.

The air temperature, measured by the temperature transmitter, ranged from 76 to 88°F. This range of temperatures corresponded to fitted temperature curves for a 15-year daily mean temperature for the Knoxville, Tennessee vicinity (Fribourg, 1976).

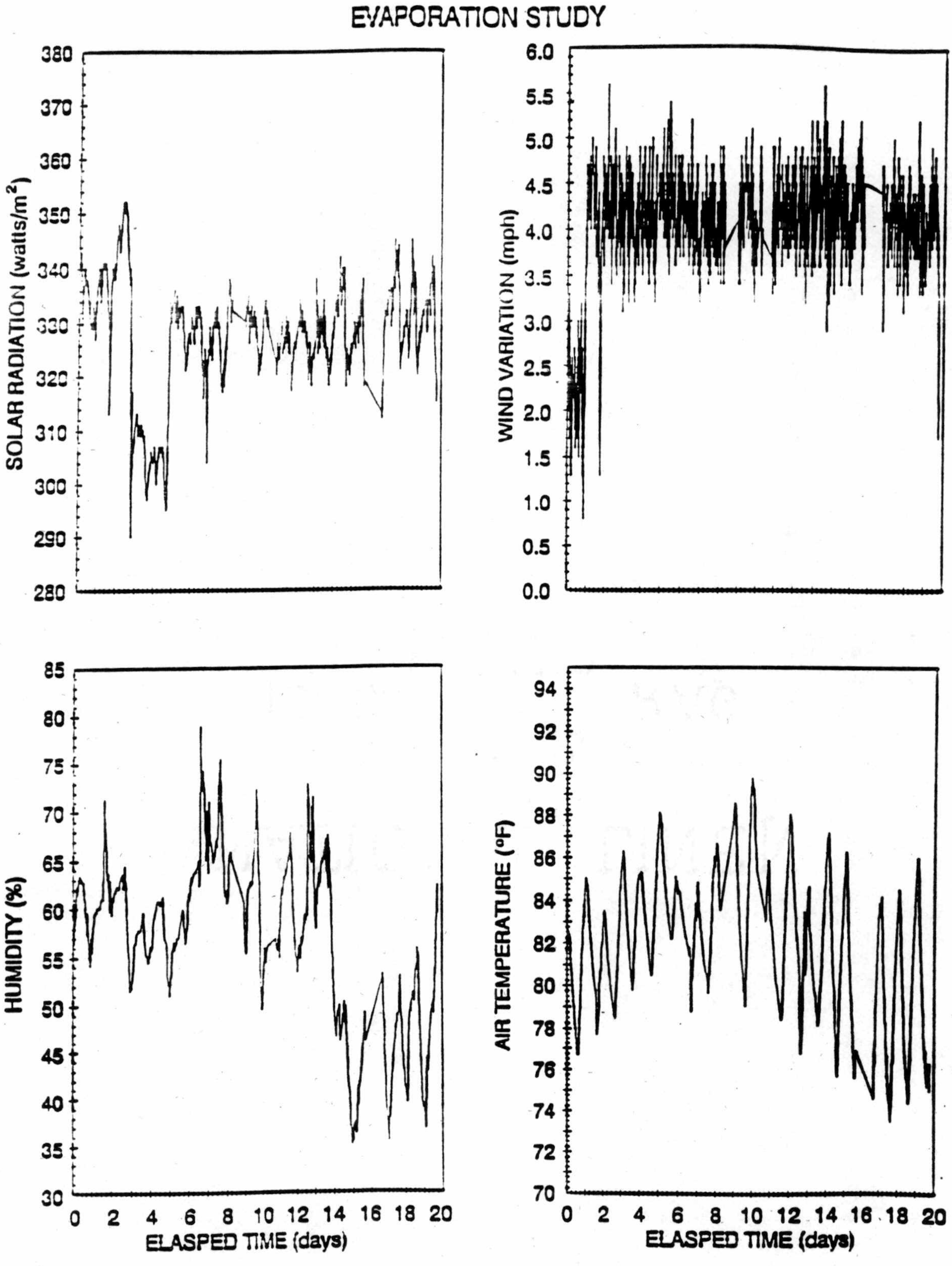

Figure 13. The 20-Day Meteorological Data Collected at the Experiment Site for Run 1.

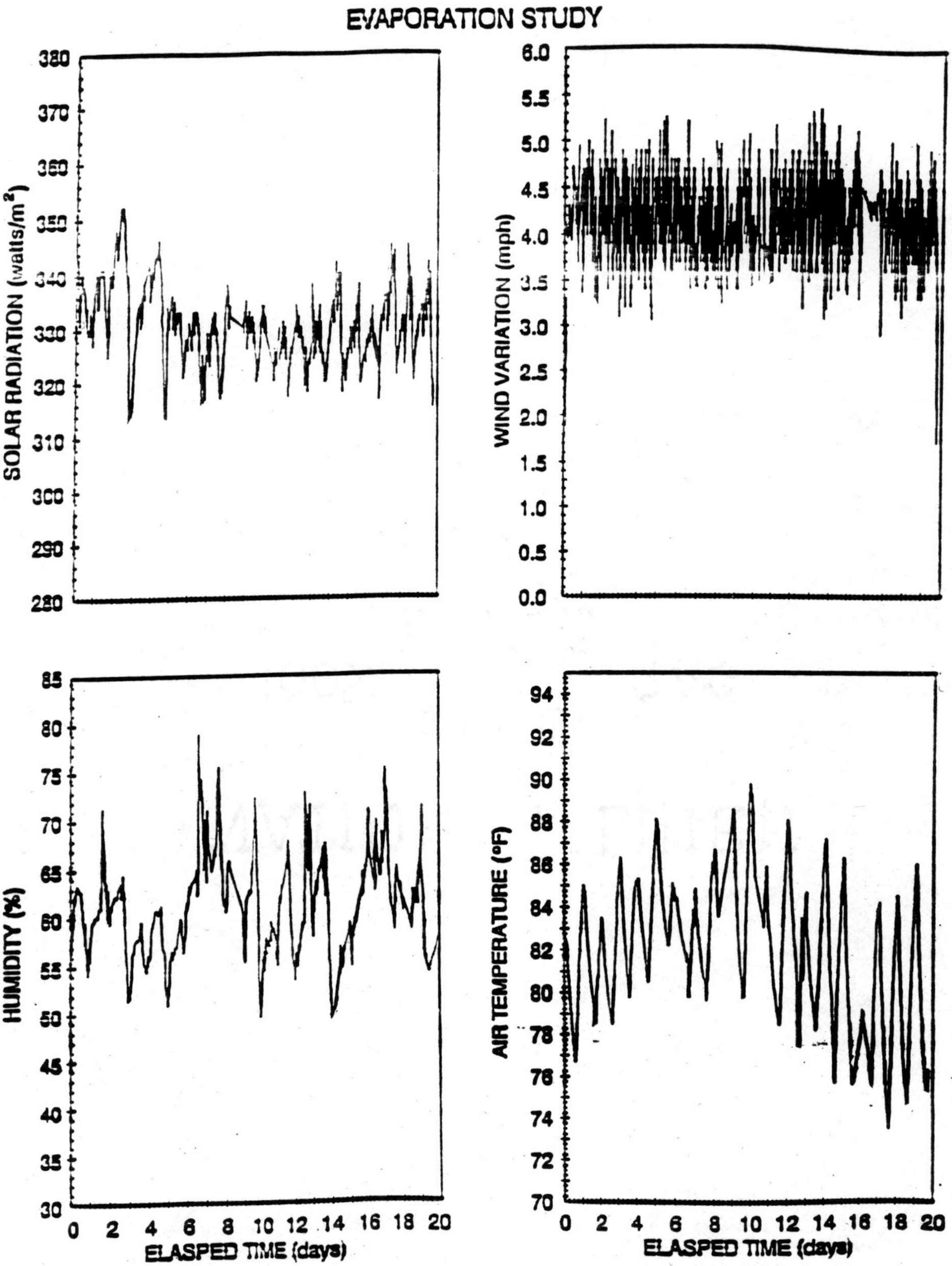

Figure 14. The 20-Day Meteorological Data Collected at the Experiment Site for Run 2.

The solar radiation value produced by the experimental setup, was approximately 330 watts per square meter. The solar radiation data recorded during the study ranged from 312 to 352 watts/m^2. Solar radiation data measured at the Blount County Farm (83° 58′ W longitude, 35° 51′ N latitude, 286 m elevation) from February 1, 1960 through September 30, 1964 and at the Plant Science Farm (84° 57′ W longitude, 35° 53′ N latitude, 253 m elevation), from October 1, 1964 through February 28, 1975 resulted in curves fitted to the 15-year daily solar radiation means, shown in Appendix A, (Fribourg, 1976). The statistical curve provided a range of solar radiation data for the Knoxville area. Based on this information the lights were adjusted to fall within this range.

Solar radiation values from the fitted curves, for the most evaporative months (April through September), ranged from 625 to 267 cal/cm^2*day. Converted to similar units measured in the study, for a comparison basis, these values were 606 and 267 watts/m^2. Based on the range, the solar radiation simulated by the light in the study, approximately 330 watts/m^2, was considered to be representative of the Knoxville area.

The change in measurements occurring during the first section of the experiment, time period of 50 to 100 hours, was due to changes in the instrumentation position and not changes in solar radiation. As discovered during run 1, the net radiometer slipped off the mounting bracket and caused an abrupt change in solar radiation. The change was a result of maladjustment and not due to changes in the experiment. Therefore, measurements during that time period were omitted because they did not represent actual conditions experienced by the ash.

Since the experiment was conducted indoors, the natural flow of wind did not occur. In field conditions wind plays an important role in evaporation by supplying a means to transport or remove vapor. To incorporate this condition, two variable-speed fans were installed to perform two tasks. The first job of the fans was to provide a cooling medium for lamps in order to reduce failure, (this aspect of the experiment is discussed in Section 6.2.2); and to provide a means to transport vapor.

Measure by a three-cup Model 430 Series Wind Speed Sensor Anemometer, the wind speed ranged from 3 to 5 mph with an average value of 4 mph. This parameter was primary controlled by setting both fans on low speed and positioning them so that the air flow was uniform.

6.0 EXPERIMENTAL LOCATION AND EQUIPMENT

6.1 General

The evaporation experiment was set up in a TVA laboratory building equipped with ventilation, electricity, and climate control. Artificial walls were constructed with plastic sheets forming a 30 x 30 ft. room housing the equipment and experimental setup. This room was constructed in order to maintain a uniform environment. The experimental setup, consisting of columns, load cells, fans, and lights is shown in Figure 15.

In the development of a complete data base, calibration tests performed by instrumentation personnel of TVA, Norris Engineering Laboratory were conducted on all equipment used in the study.

Data measured during the experiment were recorded every five minutes for the first hour and then every 20 minutes over the remaining time period. The experiment ran continuously for a period of 20 days in order to simulate a constant environment.

6.2 Instrumentation and Equipment

Equipment used to measure meteorological parameters from the column evaporation experiment and record the data required to evaluate the models consisted of the following:

1. humidity/Temperature Transmitter
2. lights
3. wind speed sensor
4. net radiometer
5. load cells
6. moisture probes and instrumentation

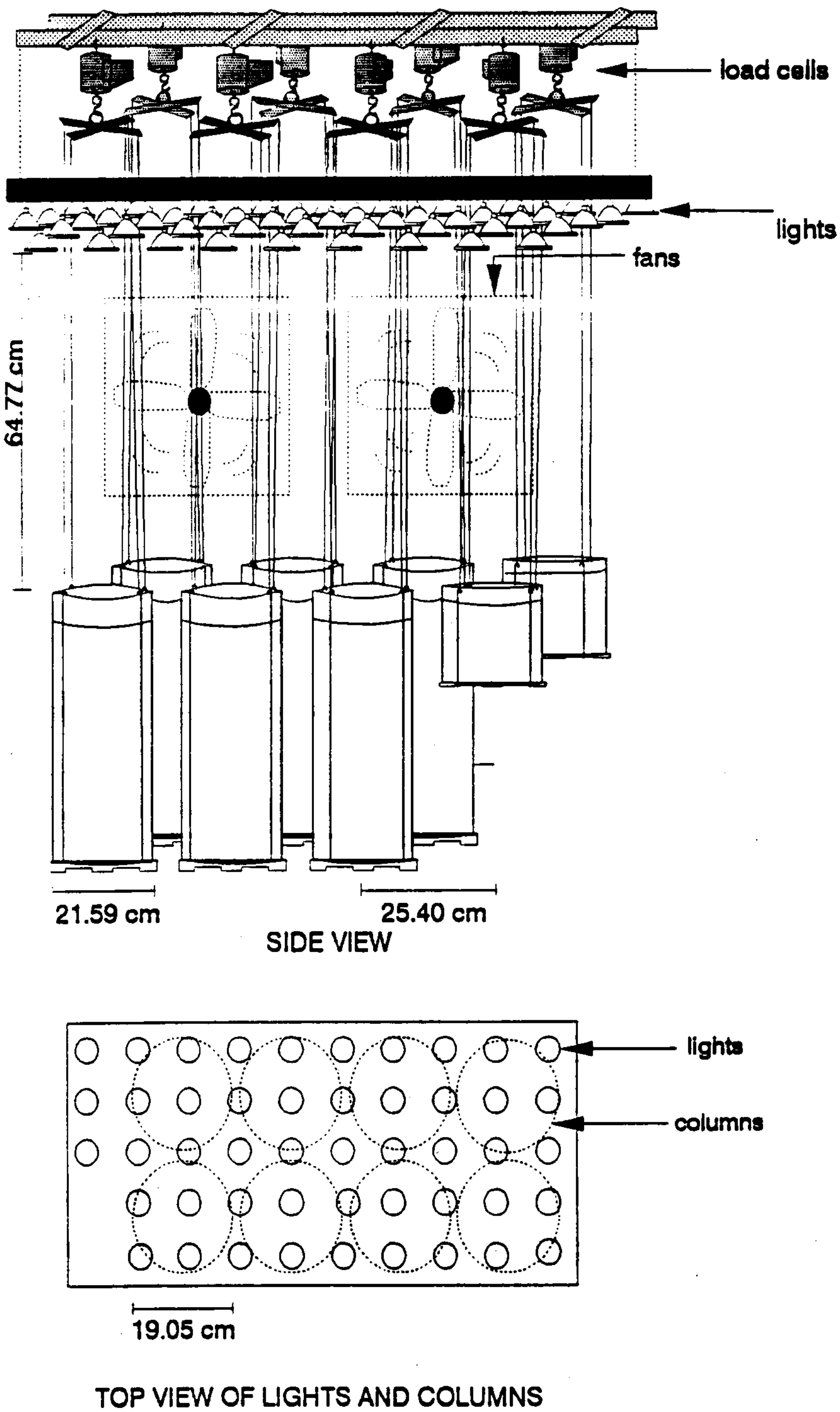

Figure 15. Experimental Setup of Ash Columns Showing Location of the Lights and Fans.

7. cylinders
8. data acquisition system

6.2.1 Relative Humidity and Air Temperature

Relative humidity is simply a measurement of the amount of moisture in the air. Practically all evaporation equations require the relative humidity and air temperature over the evaporating surface. Since the degree of saturation in the air affects the amount of water that can be removed from the surface, due to the vapor pressure gradient, the establishment of humidity and air temperature values to determine the potential for evaporation is important.

The relative humidity and ambient air temperature of the evaporating surface were monitored and recorded at the experiment site. Measurements of these parameters were accomplished using a CT-839-A humidity and temperature transmitter manufactured by Hy-Cal Engineering. The device measures temperature and relative humidity with a single probe contained in a moisture resistance housing. Temperature is determined by a thin-film, platinum, resistance temperature detector; humidity is measured with a Survivor II humidity sensor built into the probe. The accuracy of the transmitter is ±2°F for temperature and ±5% for relative humidity.

6.2.2 Lights

Since the experiment was conducted indoors, special lighting was required in order to simulate solar radiation (sunlight) for the experiment. Based on the best available technology and availability, a quartz halogen dichroic mirror lamp was selected for solar simulation. One unique feature of the lamp was that the amount of solar radiation emitted could be controlled by adjusting the operating voltage. This was possible because the lamps were constructed with a filament and a halogen burner. Based on solar radiation requirement, 330 watts/m^2, the lighting arrangement consisted of 48 lamps positioned 70 mm apart (east to west) and 65 mm apart (north to south) measured center to center of each light (each light). Equipped with its own mounting bracket, was connected to a rectangle stationary metal frame positioned 65-cm above the evaporating surface. In order to achieve a uniform lighting distribution each lamp received approximately 10 volts. To maintain a uniform environment, by preventing light failure due to overheating, a cooling medium was created by passing air over the lights. This cooling medium was accomplished by positioning two variable speed fans directly adjacent to the light roughly three feet away.

6.2.3 Wind Speed Sensor

Because of the location of the experiment (indoors) the flow of natural wind did not occur. In order to simulate wind at a constant speed, the fans previously mentioned for cooling the lights served an additional role of wind simulation. These fans provided enough wind over the evaporating surface to keep the overlying air from becoming saturated (moist air). Since the evaporation process removes water from the surface to the atmosphere because of a vapor pressure gradient, a transport medium for vapor, creating a gradient was necessary.

Wind speed created by the fans was measured with a 3-cup Model 430 Series Wind Speed Sensor Anemometer. A magnet on the rotor shaft of the anemometer generated an output pulse rate proportional to the wind velocity. To properly measure the wind speed, the anemometer was positioned on a tripod directly in front of the cylinders at the same height of the columns.

4.2.4 Net Radiometer

The light used in the experiment emitted solar radiation to the surface of the ash. In order to capture the intensity of the solar radiation or net radiation felt by the ash surface a net radiometer was used. The net radiometer, Model 3032, measured the difference between incoming and outgoing radiation of wavelengths from .3 to

60 microns. The instrument was placed between the cylinders at approximately the same height as the surface of the ash in the columns. Solar radiation values were collected in the same time frame as mentioned at the end of Section 4.1.

6.2.5 Load Cell

The experiment was designed to remove water from the cylinder by evaporation. The amount of water removed from each cylinder was determined by changes in weight. These weights were monitored and recorded by connecting a load cell (weight measuring devise) to each cylinder. Classified as a force transducer, the load cell converts the force or weight into an electrical signal. A resistance strain gage bonded to an elastic strain member that followed the deformation of the load created the electrical signal. Once any change in weight was detected by the load cell, an electrical signal was transmitted to a data recorder. The data recorder converted the signal back to a weight measurement and stored the information throughout the experiment. The rated capacity of the load cells ranged from 50 to 100 pounds, with an overload rating capacity of 150%.

6.2.6 Moisture Probe and Instrumentation

An additional aspect of the experiment was to measure the moisture profile of the fly ash in the columns throughout the evaporation experiment. These measurements would provide a means of identifying the location or zone in which water movement occurred. These data would provide insight to the height of capillary rise exhibited by the ash. Unfortunately, no measurement technique of soil water content in the study of unsaturated water flow has been documented as the preferred method. Some common methods used to measure moisture content of soils are: electrical resistance (Bouyoucos and Mick, 1940), gamma ray absorption (Ferguson and Gardner, 1961), and neutron moderation (Long and French, 1967). Although these procedures are all valid methods for measuring soil moisture, the method chosen was Time-Domain Reflectoretry (TDR) based on availability of instrumentation and mobility of use.

The TDR theory is based on the dielectric properties of the material and is dependent on homogeneous properties. This technique measures the volumetric moisture of the material by placing two parallel, stainless steel probes in the ash, approximately two inches apart in the horizontal plane. The moisture readings were provided by a Trase System, Model 6050X1 manufactured by the Soil Moisture Equipment Corporation. The Trase system instantaneously measures the volumetric moisture by averaging the time required for a microwave pulse to travel down the transmission line. The Trase system (Figure 16) consists of weather proof housing for instrumentation, wave guides, and a Trase wave guide connector. Unfortunately, the Trase System has not been tested on fly ash and does not give conclusive data on soil moisture measurements taken within the ash columns.

6.2.7 Cylinders

In order to create a condition that would minimize horizontal movement and allow vertical movement it became necessary to store the fly ash in a leak proof container. This container was not intended to encourage upward movement (capillary rise due to the diameter of the container) but allowed it to occur based on the hydraulic properties of the material (Colbert and Kingston ash). Since the weight of each container was monitored throughout the experiment, preventing the leakage of water was important. The container selected was a hallow circular acrylic cylinder. This type of container would reduce the amount of potential leak areas by minimizing assemblage, while providing a means of storing and positioning the ash.

Eight circular acrylic cylinders, 17.8-cm in diameter, 46-cm in height, and .635-cm thick, were constructed for the first evaporation test. Another 4 cylinders, 17.8-cm in diameter, 91-cm in height, and .635-cm thick were

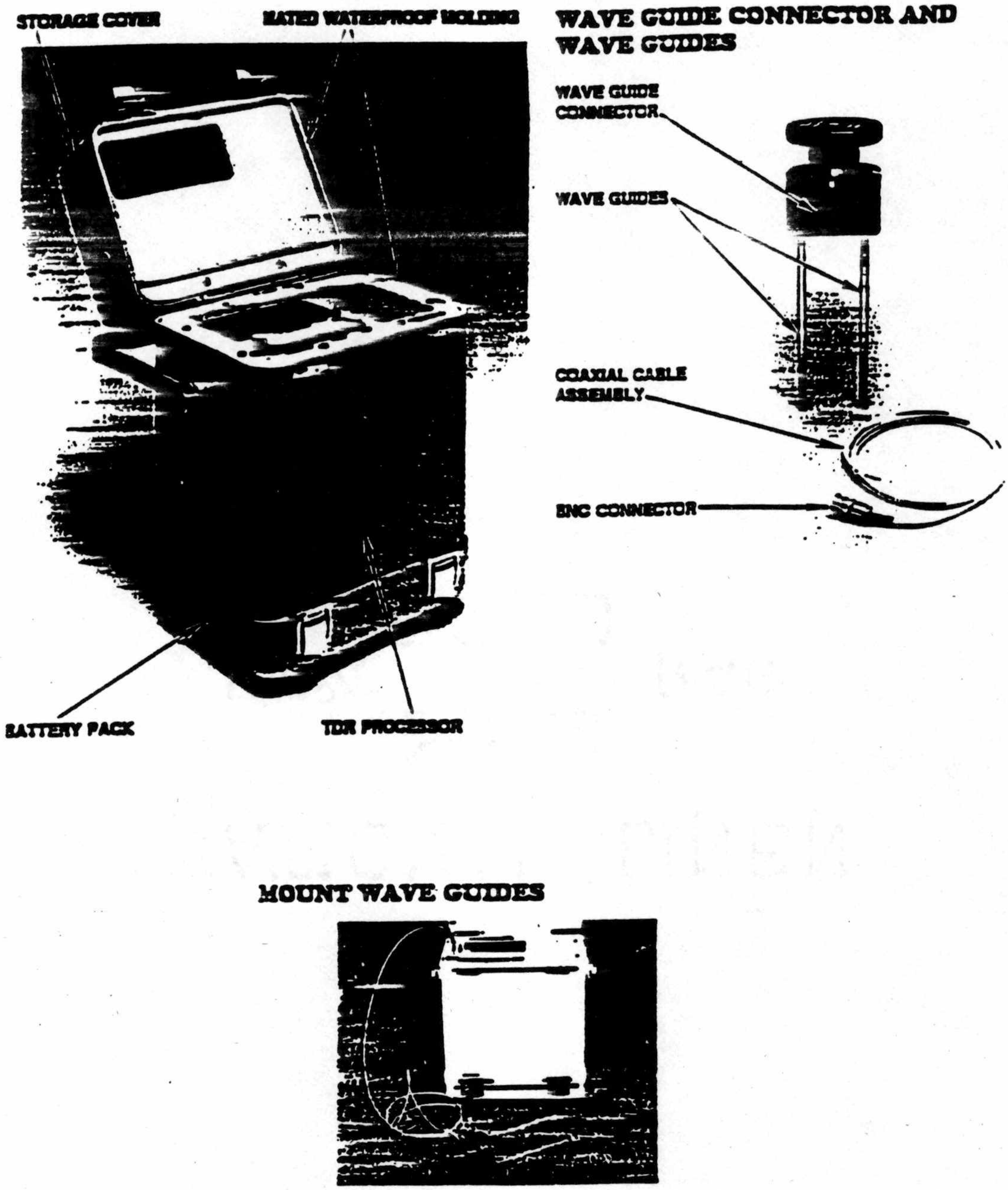

Figure 16. Trase System Used to Measure Moisture in the Ash

constructed for the second evaporation test. The cylinders were modified by drilling six holes (used to insert the wave guides to measure moisture) in the side and placing mounting brackets on the sides for hanging (Figure 17).

6.2.8 Data Acquisition System

A data acquisition system provided the ability to record and access a data base of information created during the experiment. The integral components of the evaporation experiment were combined by an HP 3852S data acquisition and control system (DACS). The DACS provided the physical means capable of measuring parameters through transducers which provided a controlled output. The system mainframe had considerable built-in intelligence that increased the speed of collecting data.

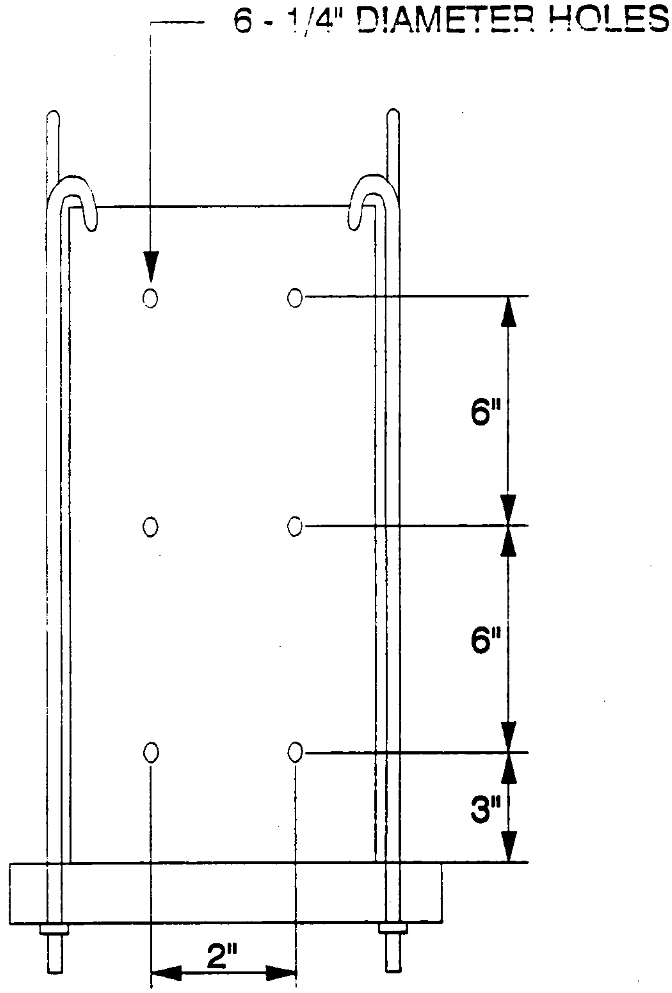

Figure 17. Acrylic Circular Cylinder Used in the Evaporation Study

7.0 EVAPORATION EXPERIMENT

7.1 General Approach

An evaporation study was conducted to generate data for validating the performance of three, one-dimensional unsaturated groundwater flow models. The experiments were designed so they would be both easy to conduct and easy to model. The study focused on measuring the evaporation rates from cylinders of fly ash that had no flow boundary conditions at their bottoms and sides and a constant evaporation potential at their tops. The evaporation experiment was estimated for a 20-day period under constant meteorological conditions (no pulsing). The constant evaporation potential reduced the effects of hysteresis and decreased the complexity of delineating stage I and stage II evaporation periods. Two experiments were conducted to evaluate the effect of the initial moisture content on evaporation processes. The first set of experiments included fly ash that was nearly saturated, while experiment 2 included fly ash that had moisture contents very similar to those typically measured in the field.

The first experiment of near saturation was a condition that rarely occurred in an actual field setting but was of theoretical interest in relation to potential evaporation. Input requirements of the numerical models included data for calculating potential evaporation. This calculation could be performed by the model or calculated beforehand and included as input. Although the HELP2 model does not require it, prior calculation of the potential evaporation is calculated within the code based on input data. Equations used to calculate PE by the models were based on free water surface evaporation. With this in mind, it is questionable that the potential evaporation of a free water surface and of the water surface of the fly ash would be identical. Some of the reasons that may affect this potential rate are that changes in the ash material could occur (clogged pores) and that free water surfaces and ash water surfaces may absorb heat differently. Therefore, it may be necessary to evaluate potential differences between the two rates.

7.2 Material Preparation

Two primary concerns with preparing the ash columns for the experiments were mixing and packing the material. Mixing was necessary to bring the moisture content of the ash to a desired level and this was performed by mechanically combining water with the ash as uniformly as possible. The amount of water added in the ash was based on the target moisture content. The target volumetric moisture contents for the two evaporation tests were approximately 42% for the first run and 22% for the second run. Mixing of the ash samples was performed using a power driven mechanical mixer, and water was added with a fine-mist spray nozzle. To assure the proper moisture contents were achieved, grab samples were taken and checked throughout the mixing process. Once the desired target volumetric moisture content was reached, the materials were sealed and allowed to set to reach moisture equilibrium within the ash. After approximately five days, the mixed samples were rechecked to assure that the targeted moisture was maintained. The volumetric moisture content reached for the first experiment for the entire Colbert sample was 43% and 35% for the entire Kingston sample. The volumetric moisture throughout the entire sample for the second experiment was 24 and 22% for Colbert and Kingston ash, respectively. When the analysis of the moisture content was completed, the materials were packed into two groups. The first group, three columns of Colbert fly ash, was packed as uniformly as possible, while the second group, also three columns, was filled with Kingston fly ash. Packing was performed by physically tamping the ash in small increments in each cylinder from the bottom up. Preventing entrapped air and achieving uniform densities and porosities similar to those used earlier in determining the hydraulic characteristics were important aspects of packing.

Since there was no equipment readily available to measure the density of the materials during packing, each cylinder was sampled at the end of the test. Sampling was preformed by separating the ash in each cylinder into 3-in intervals. Each ash sample was placed in a properly labeled container. The samples were weighed and dried for 24 to 48 hours at 310°F and reweighed. The sectional sampling also provided a snapshot of the moisture profile. Figures 18 and 19 represent the moisture, density, and porosity profiles of the Colbert and Kingston fly ash, respectively. The results indicated that uniform densities and porosities comparable to those used in the hydraulic measurements test performed by Daniel B. Associate could be achieved from a relatively primitive and inexpensive procedure. The variation in densities and porosities was attributed to entrapped air but was not considered significant. However, the moisture profile data indicated that column length was an important parameter that needs additional study.

The material contained in the columns was expected to experience a drying front. Similar in concept to a wetting front, this front was to proceed downward to a depth not limited by the cylinder length. The column length for experiment 1 was 46-cm, but as a result of the strong capillary forces of the ash, the drying front exceeded the length of the column and consequently limited the availability of water. Because of bottom boundary conditions, the actual evaporation data could not be compared to the result of the WF model. Yet the bottom boundary condition could be corrected by increasing the length of the cylinder to 91-cm and was performed by

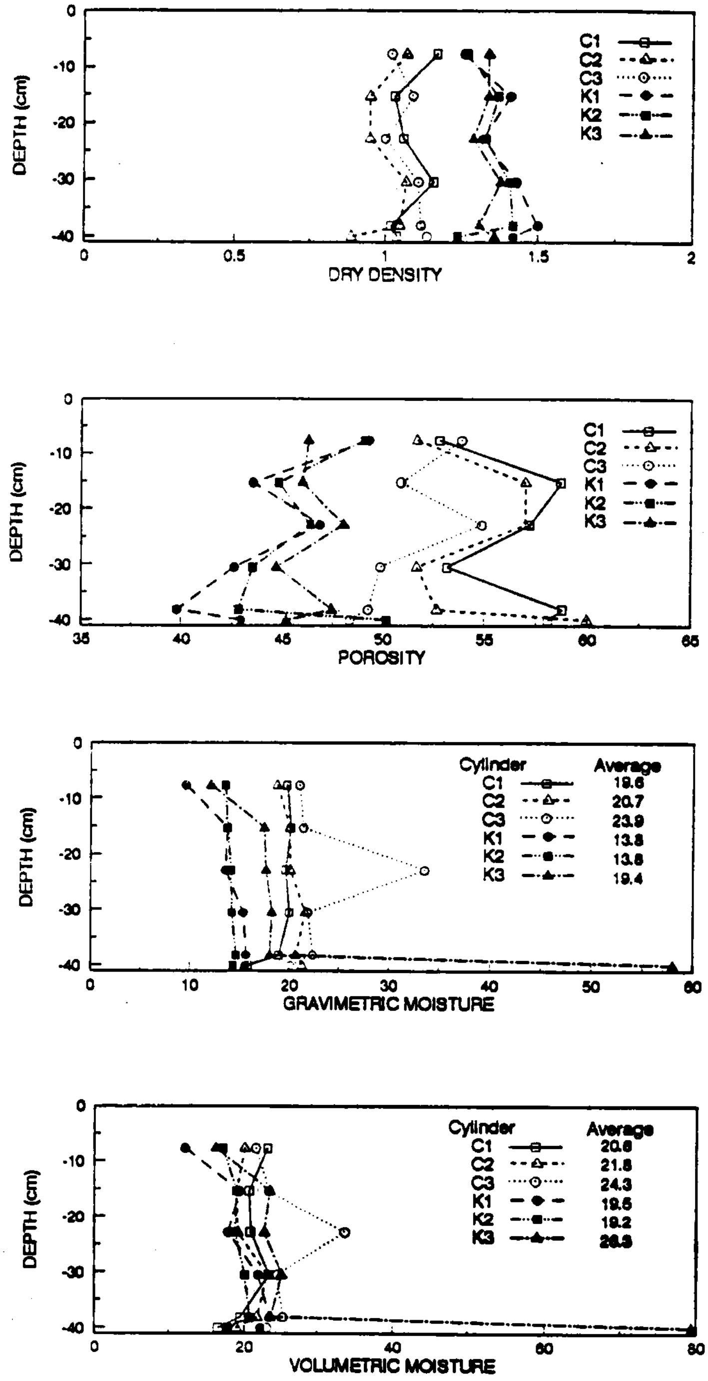

Figure 18. Measurements of Moisture, Density, and Porosity Profile Throughout the Column of the Colbert Fly Ash for Run 1

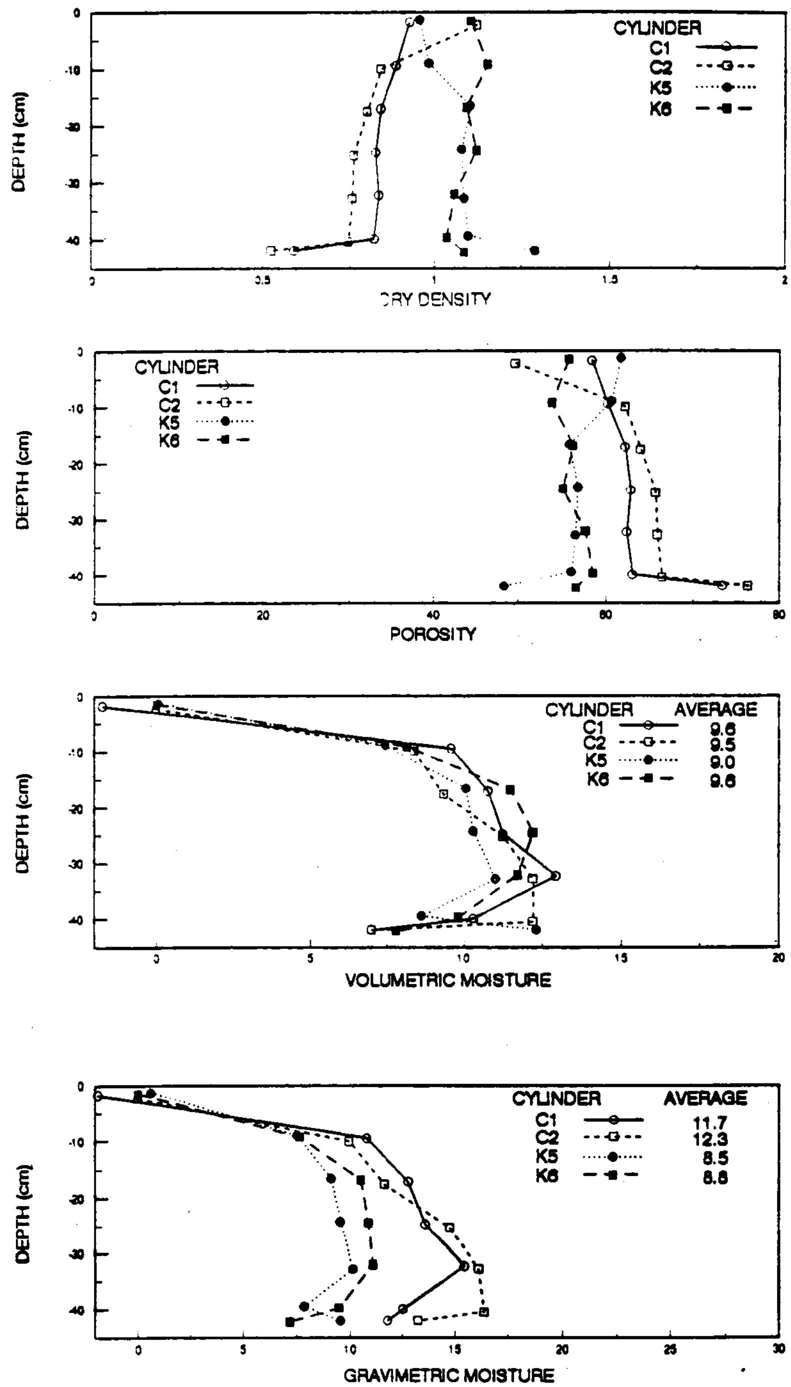

Figure 19. Measurements of Moisture, Density, and Porosity Profile Throughout the Column of the Kingston Fly Ash for Run 2.

conducting an additional experiment.

7.3 Potential Evaporation

Of the various parameters considered in the models one of primary interest was potential evaporation. In order to evaluate two of the numerical models (WF and UNSAT1D) the potential evaporation rate needed to be calculated or measured. The third model (HELP2) internally calculate the potential evaporation rate based on climatological data. The potential evaporation rate simulated by the experiment was measured to be approximately .88 cm/day. The potential evaporation created by the experimental setup was measured three ways: a free water surface evaporation test and a saturated fly ash (Colbert and Kingston) test; and calculation using the modified Penman's equation.

A run to measure potential evaporation (PE) from a free-water surface was conducted with six cylinders of water under the same experimental setup used to conduct the fly ash experiment. Following completion of experiment one, fly ash cylinders were replaced with identical cylinders containing potable water. The columns were connected to the same load cells and monitoring equipment. It was assumed that the PE rate imposed by the laboratory setup could be determined by measuring the weight loss of each cylinder. The test ran for 14 days; water removed from each cylinder by evaporation was replaced every two days to keep the water level near the surface. Based on the results or the weight measurements from the free water evaporation run the PE rate ranged from .88 to .91 cm/day, with the middle cylinders being the highest. Based on intermediate measurements taken from each cylinder during experiment 1, it was assumed that the middle cylinders encountered higher wind speed and more solar radiation. This may explain the increase in evaporation for the middle cylinders.

A run to measure the PE rate from both Colbert and Kingston fly ash near saturation was performed at the same time experiment 1 was being conducted. In order to keep the ash near saturation, a special container was constructed. The container, shown in Figure 20, consisted of a water proof rectangular box (used to store water), with a circular cylinder filled with multiple holes for water passage, positioned in the center to keep the water and ash separated but allow passage of water to the ash. The measurements and time period were identical to that of experiment 1 since they were conducted simultaneously. It was assumed that the PE rate imposed by the setup could again be determined by measuring the weight loss of each cylinder. Based on the results of the weight measurements of the saturated ash, the Colbert fly ash revealed a PE rate of .89 cm/day and the Kingston ash .88 cm/day. The difference in the evaporation rate was negligible but could be contributed to differences in hydraulic properties.

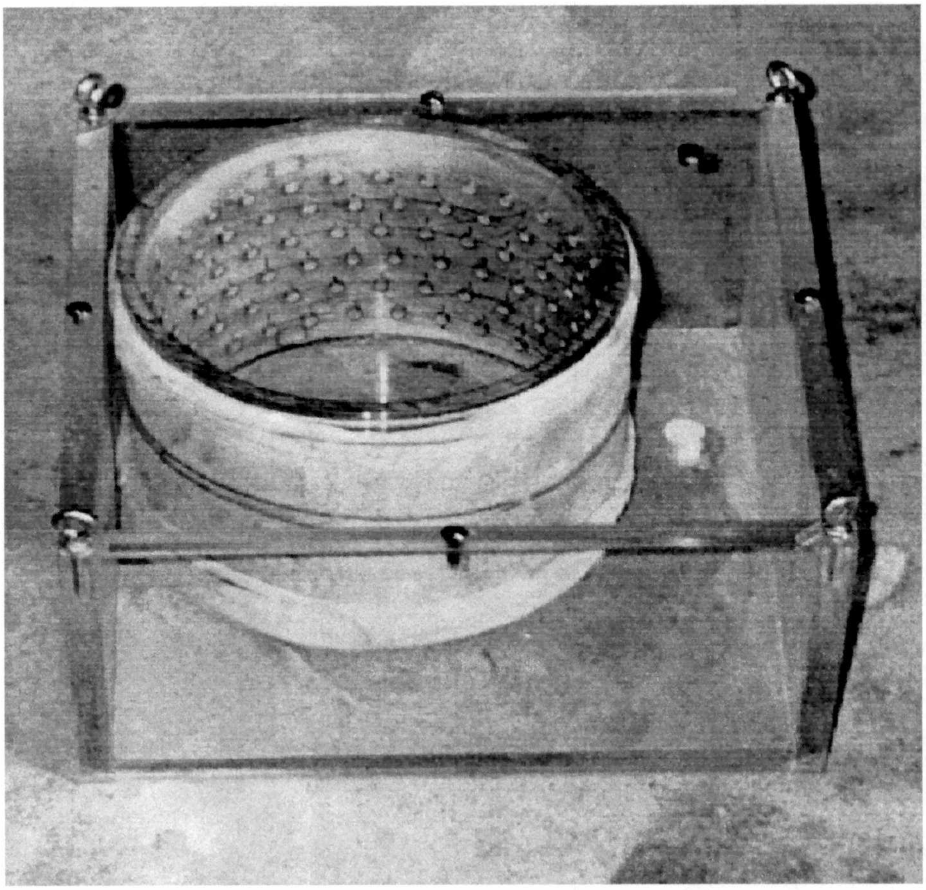

Figure 20. Container Used to Achieve and Maintain a Saturated Condition in the Fly Ash for Experiment 1.

Based on the meteorological parameters of the experiment, the potential evaporation rate was approximately .89 cm/day and was made using the modified Penman's equation. The equation is given as:

$$P.E. = \frac{1.28}{2.54} * \frac{S}{S+Y} * Qne \qquad (42)$$

where:

P.E.= potential Evaporation (in.)
Y = psychometric constant (.68 mb/°K)
Ts = surface Temperature (°K)
Ta = air Temperature (°K)
S = slope of the saturation vapor pressure curve
Qne = incident solar radiation (langley)

7.4 Experiment 1

The first evaporation experiment was initiated on May 21, 1991, and finished on June 7, 1991. The experimental site and equipment used to measure the parameters involved in the study were those described in Section 6.0. The first test consisted of six columns of fly ash divided into two groups of three columns each. The first group (columns 1, 2, and 3) was filled with Colbert fly ash with a volumetric moisture content of 44%. The second group (columns 4, 5, and 6) was filled with Kingston fly ash with a volumetric moisture content of 35%. The material used in the study was prepared as described in Section 6.1. Once the cylinders were packed, all columns were sealed and allowed to set approximately 48 hours to reach equilibrium within the column. The columns were then subjected to a constant potential evaporation rate.

Also included in the setup were two additional containers used to simulate near-saturation conditions in the ash. These containers and saturated experiments were previously discussed in Section 7.3.

During the evaporation test, weight measurements were continuously recorded using load cells occasionally, calibration of the load cells was checked by physically removing each column from the load cell. Each column was weighed on a digital scale and returned to its original position. Weight measurements were taken approximately two times a week over the 20-day period. The weight measurements taken from the scale compared with weight measurements recorded by the load cells and are graphically presented as cumulative evaporation (cm) in Section 8.1.

Volumetric moisture measurements throughout the experiment were taken approximately every two days over the 20-day period using the Trase System. These measurements were taken to provide a snapshot of moisture movement in the ash during the experiment. Calibration tests performed on the machine before the experiment began concluded that, under wet conditions (greater than 30% moisture by weight), the dielectric properties of the ash changed and disrupted the electromagnetic pulse generated by the machine. However, the Trase system appeared to predict the moisture content of the ash for moist conditions (less than 30% gravimetric moisture).

Upon completion of the experiment, volumetric moisture measurements were taken to determine the depth of drying and provide additional comparisons to the Trase moisture measurements. Volumetric moisture measurements require knowledge of the volume, initial weight and final weight of the ash. These measurements were taken by sectional sampling as previously described.

The moisture profiles provided by sectional sampling indicated that drying occurred throughout the entire column length. As a result, the amount of moisture removed was limited by boundary conditions. Because of these conditions, the WF model was not applicable, and an additional test was performed.

7.5 Experiment 2

The second experiment was performed under the same environmental conditions as the previous experiment. The material preparation, calibration tests, and individual measurements taken in the first experiment were also performed in the same manner in the second experiment. The columns used in the second experiment were positioned in the same location (i.e., the Kingston columns closest to the fans) as the previous test. Changes in the second test consisted of lowering the volumetric moisture contents to 22 and 24% (similar to field conditions) in the Colbert and Kingston ash samples, respectively, and using only four cylinders. Since the setup only consisted of four columns, the two center positions were empty.

The four columns used in the second experiment formed two groups. The first group contained two 46-cm columns, one filled with Colbert fly ash and the other filled with Kingston fly ash. These columns were used to obtain additional information on the evaporation coefficient and to check for any changes due to drying, such as surface crusting or salt accumulation. The second group included two 91-cm columns. Again, one column was filled with Colbert fly ash while the other contained Kingston fly ash. The longer columns prevented bottom-boundary conditions and provided enough length to accommodate capillary forces displayed by the fly ash. The moisture profile of the second experiment was lower and more similar to field conditions. Since dry stacking usually occurs at moisture contents from 18 to 24%, the data obtained would provide a better comparison to field situations.

8.0 RESULTS

8.1 Actual and Model Results from the Evaporation Experiment

The primary purpose of the study was the comparison of modeled evaporation predictions to the actual measured results. To provide the necessary input parameters the same measured climatological data base used by all three models was constant. Likewise, the same set of measured hydraulic properties of the Colbert and Kingston fly ash were used. Since none of the models account for hysteresis in the unsaturated properties of the materials, model simulations were performed using the IDC data. The IDC data was used because it closely resembled the same conditions being simulated during the experiment (i.e., moisture content of the material increased to near saturation and then allowed to dry).

The measured cumulative evaporation from experiment 1 using 46-cm columns with Colbert and Kingston fly ash are shown in Figure 21. Plotted in this figure is the actual cumulative evaporation (cm) as a function of time (days). The cumulative evaporation for experiment 1 is plotted as a separate figure because the materials are assumed to be independent of each other. The cumulative evaporation of the second experiment, shown in Figure 22, includes both 46-cm and 91-cm length columns. The four columns used in the second experiment contained two columns with Colbert fly ash and two columns with Kingston fly ash.

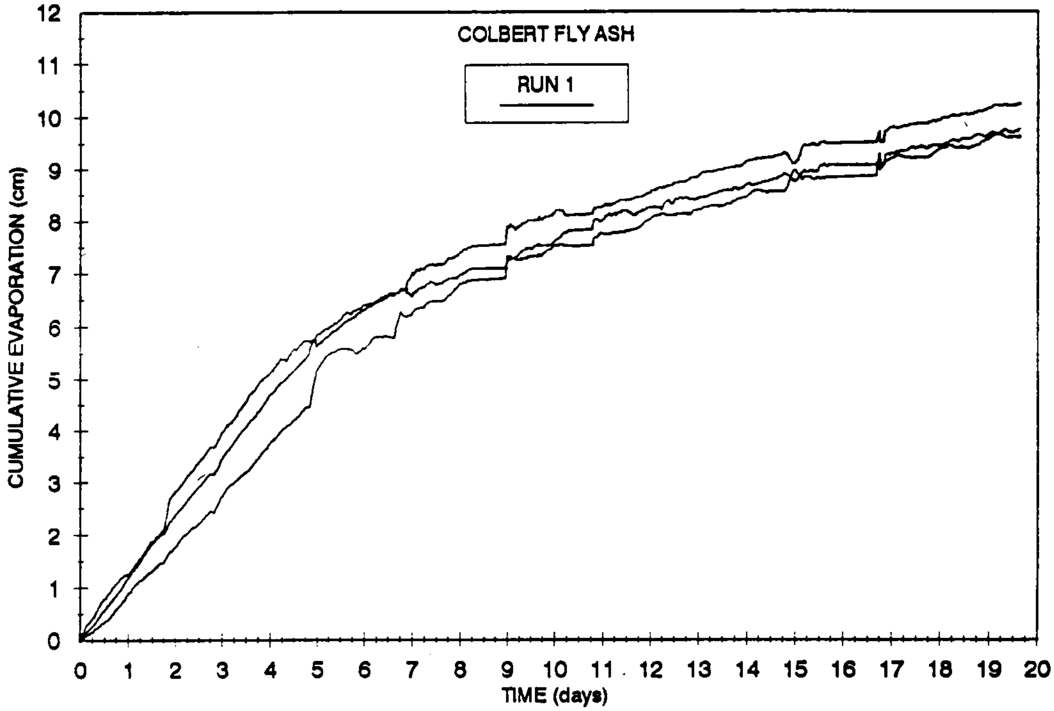

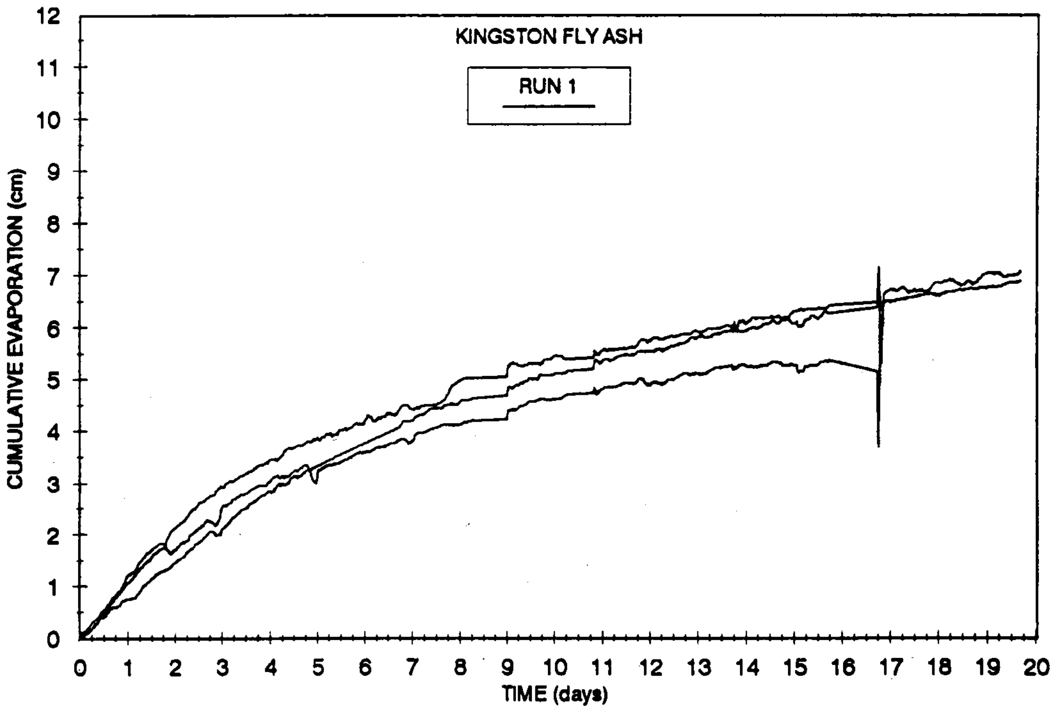

Figure 21. Cumulative Results of the 20-Day Column Evaporation Experiment for the Colbert Fly Ash Group and the Kingston Fly Ash Group, Respectively for Run 1.

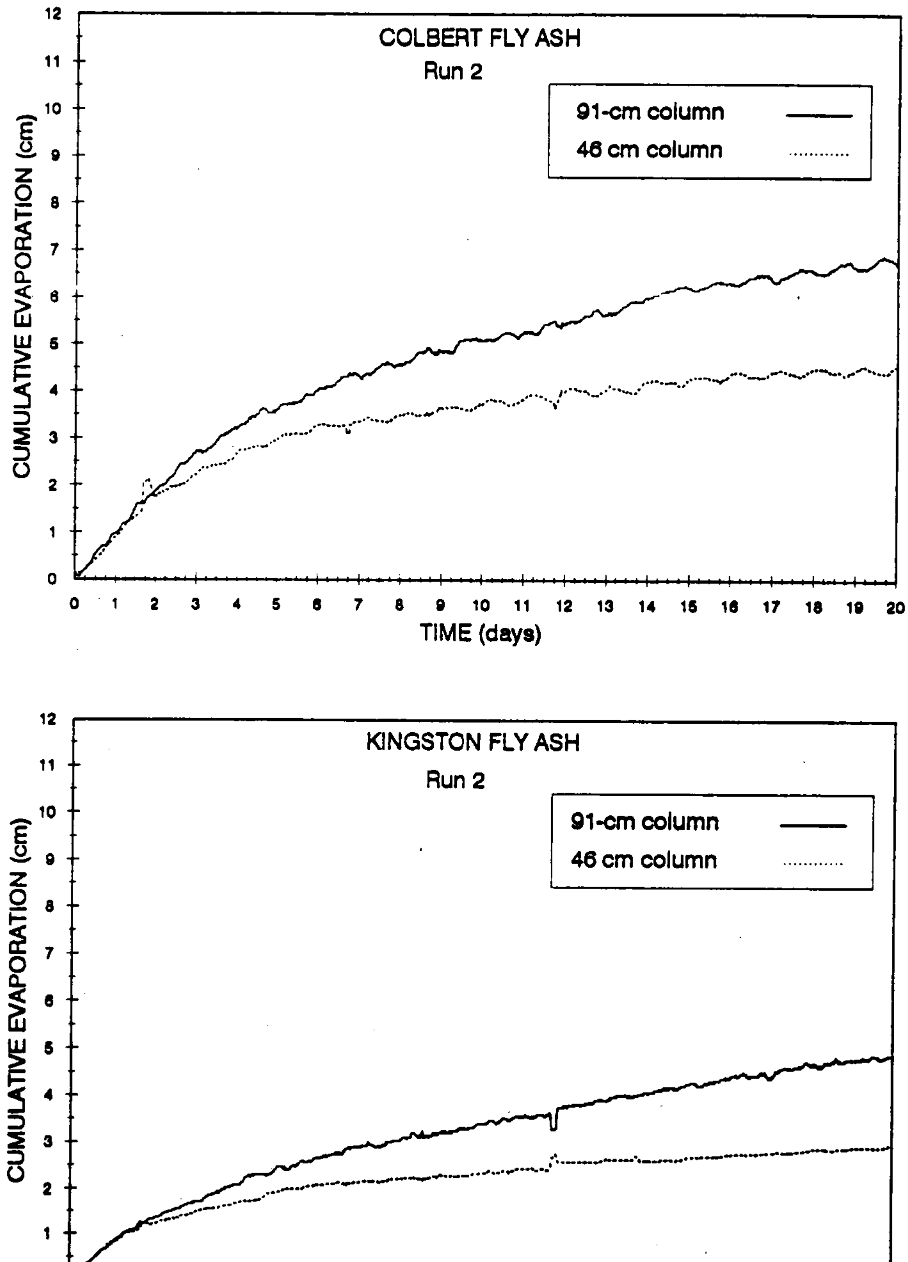

Figure 22. Cumulative Results of the 20-Day Column Evaporation Experiment for the Colbert Fly Ash Group and the Kingston Fly Ash Group, Respectively for Run 2.

Results of the second experiment showed that the initial moisture content and the column length affected the amount of water removed by evaporation.

Because the first experiment was run using 46-cm columns, the WF model could not be applied. This exemption of the WF model stems from the assumption of a semi-infinite profile used in developing the code. Evaluation of the model reveals a moisture discontinuity termed the wetting front. This wetting front descends into the profile having a semi-infinite depth dependent on the hydraulic properties. The 20-day simulation using the 46-cm columns was insufficient in providing enough depth to evaluate the WF model properly. Analyzing the moisture profile from experiment 1 showed that additional length should be added to properly evaluate the model. Length was added by replacing two 46-cm columns with two 91-cm columns in the second experiment. The deeper cylinders appeared to be sufficient to provide a data set capable of evaluating all the models.

Because the columns experienced variable (spatial) climatological conditions, only two data sets (one Colbert and one Kingston) were selected. The data sets consisted of one 91-cm column filled with Colbert fly ash and one 91-cm column filled with the Kingston fly ash used in the second experiment. These cylinders provided a basis for comparing all three models; they also experienced meteorological conditions similar to the target data. The results of the actual data compared to the modeled results were shown in Figures 23 and 24. Since all three models are compared for simultaneous runs, the conclusions drawn are based on the longer columns.

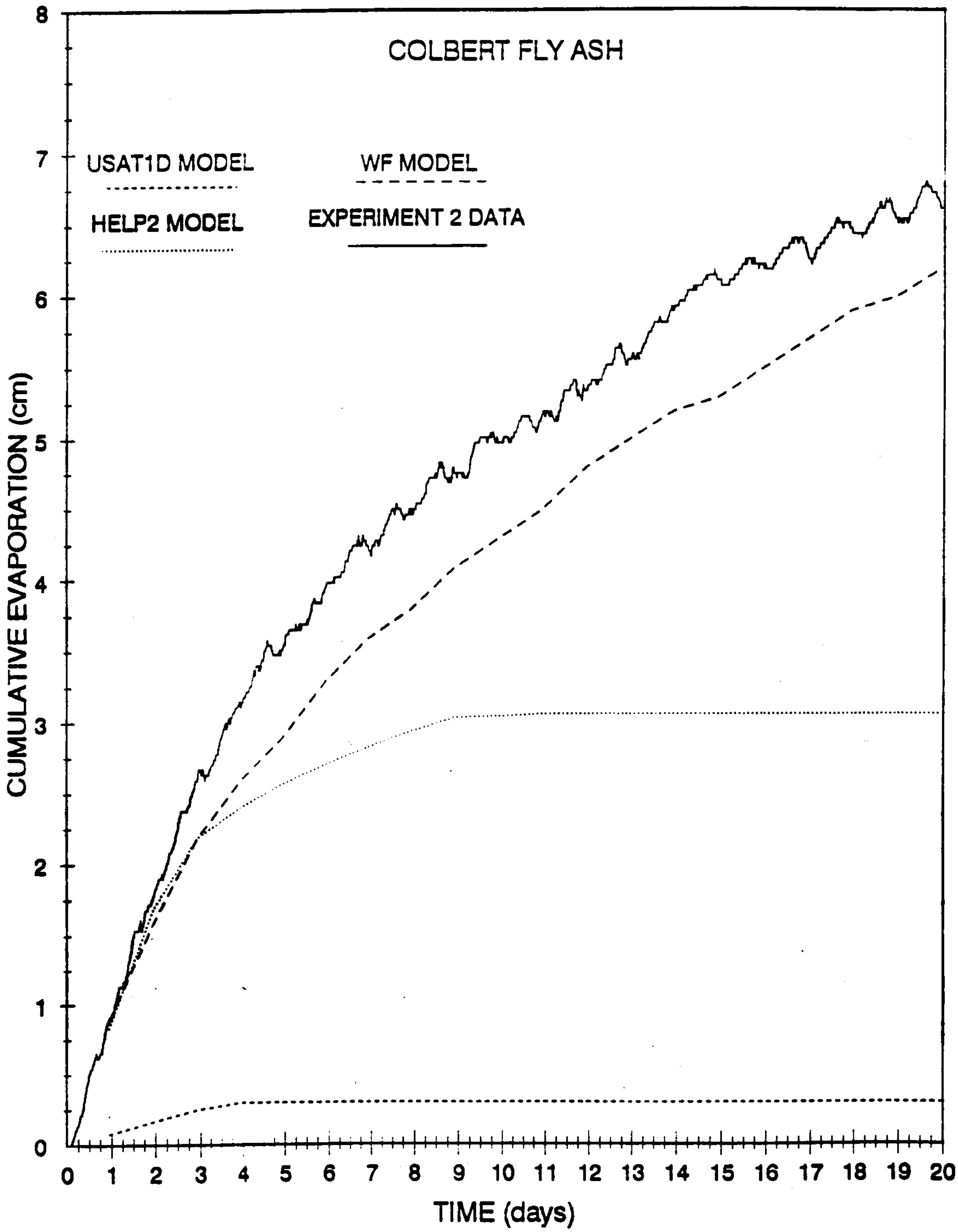

Figure 23. Comparison of Measured and Modeled Results of Experiment 2 for Colbert Fly Ash.

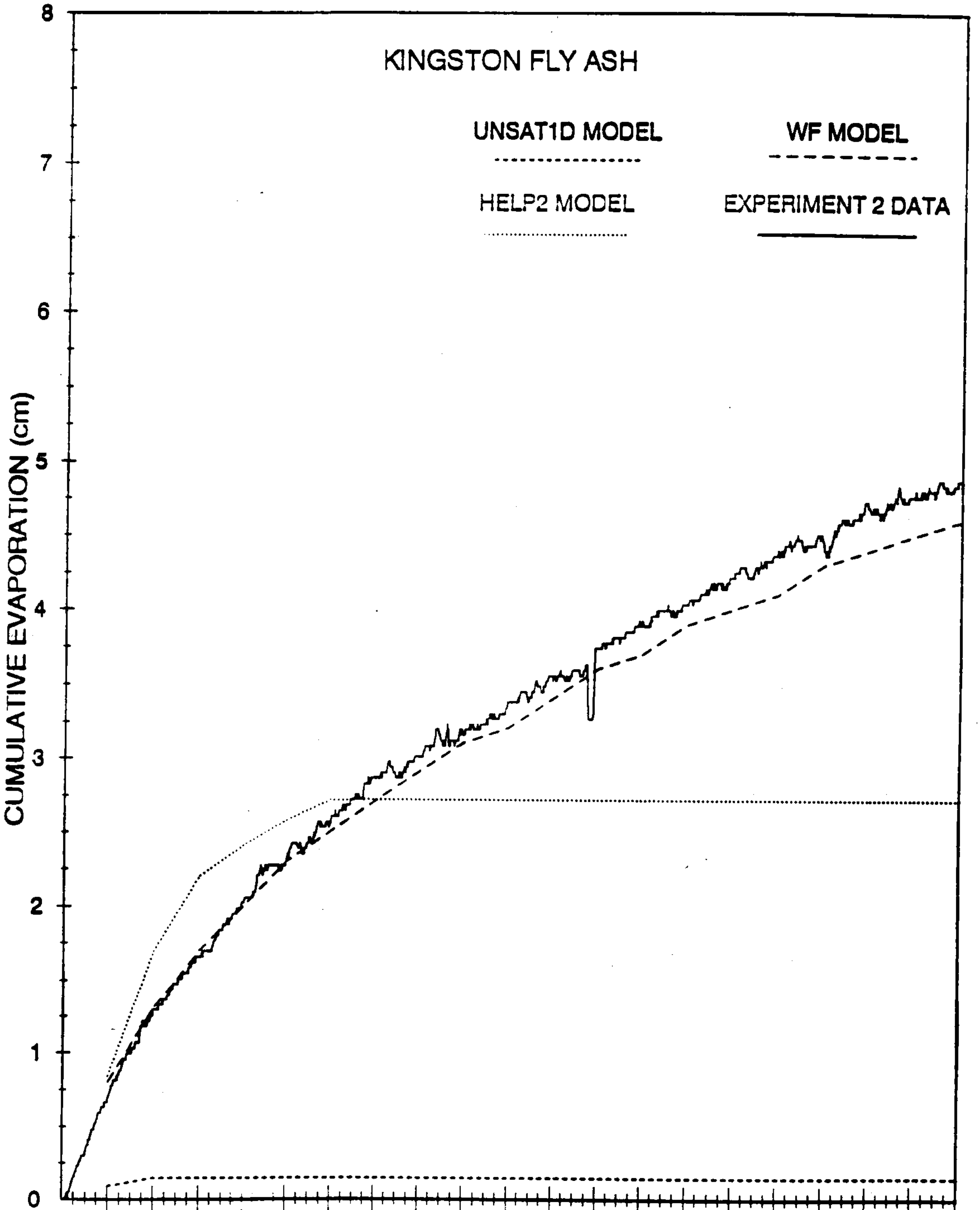

Figure 24. Comparison of Measured and Modeled Results of Experiment 2 for Kingston Fly Ash

9.0 DISCUSSION OF RESULTS

9.1 Model Evaluation

As described in Section 7.0, a column evaporation study was conducted, to test three numerical water budget models. Based on the experimental data, the evaporation routine of the 3 models were tested by comparing weight changes in the column, determined to be evaporation to computer-simulated values from UNSAT1D, HELP2, and the Wetting Front Model. Values of the measured experimental evaporation and computer-simulated results for Colbert and Kingston fly ash are shown in Tables 2 and 3, respectively. The evaporation predictions of the three models differed significantly. The noticeable differences between the values after day 1 were primarily due to the shift from stage 1 to stage 2 evaporation.

Table 2. Summary of Cumulative Actual versus Model-Predicted Evaporation of Colbert Fly Ash from Experiment 2

Actual and Simulated Evaporation				
Day	Actual Evap. (cm)	WF (cm)	HELP2 (cm)	UNSAT1D (cm)
1	0.914	0.900	0.846	0.089
5	3.546	2.900	2.576	0.309
10	4.972	4.300	3.053	0.309
15	6.106	5.300	3.066	0.309
20	6.617	6.200	3.066	0.309

Table 3. Summary of Cumulative Actual Versus Model-Predicted Evaporation of Kingston Fly Ash from Experiment 2

Actual and Simulated Evaporation				
Day	Actual Evap. (cm)	WF (cm)	HELP2 (cm)	UNSAT1D (cm)
1	0.695	0.800	0.846	0.089
5	2.340	2.300	2.576	0.149
10	3.364	3.200	3.053	0.149
15	4.204	4.000	3.066	0.149
20	4.862	4.600	3.066	0.149

All three models used in the experiment underestimated evaporation during the simulation period. However, it was evident from the data that the WF model from experiment 2, having 91-cm columns, showed the best overall comparison with the actual evaporation results.

9.1.1 UNSAT1D

The cumulative evaporation predicted by UNSAT1D was approximately 95 and 97% less than the observed evaporation for the Colbert and Kingston fly ash, respectively, by the end of the study period. It was likely that the simulated UNSAT1D results grossly underestimated the evaporation for two reasons. The first explanation was based on the algorithm used to calculate evaporation. The model used equation 18, derived from a study by Beese etal. (1977). From field research, Beese determined an empirical relationship between potential evaporation, actual evaporation, and soil suction. This relationship, previously shown in Figure 8, was the methodology incorporated by the model. According to the analogy, the evaporation rate is inversely proportional to the suction head at the surface node. For any suction heads less than 30-cm, the model evaluated an evaporation rate equal to the potential. For suction heads greater than approximately 900-cm, the model computed an evaporation rate of 10% of the actual evaporation. Since the model consistently underestimated evaporation in all tests performed on the ash, the evaporation characteristics of the fallow loessial soil did not appear to be representative of the specific waste material being considered.

The second reason evaporation was underestimated by UNSAT1D was because the model was sensitive to the user-defined grid spacing. Each column was describe by a series of incremental vertical elements of a given thickness defined by the user. A grid spacing of 4-cm was defined for modeling the fly ash columns. The 4-cm spacing was considered to represent both the infiltration and evaporation processes.

The model assumed that water in the form of precipitation or irrigation entered the surface and migrated downward. The water was then removed from the profile at a depth defined by the grid-spacing. When the moisture was removed from the surface nodes this caused the top layer to become dry. This in turn initiated the upward movement of moisture from underlying layers due to a moisture gradient. However, this upward movement of moisture was very slow, and in fact, very little water was removed until another wetting front was encountered. Along with the methodology used to calculate evaporation, this process helped explain the small amount of evaporation simulated by UNSAT1D model.

9.1.2 HELP2

At the end of the study the evaporation predicted by HELP2 was approximately 53.6% less than the observed evaporation for the Colbert and 36.9% less than the observed evaporation for the Kingston fly ash. The results from the HELP2 simulation indicated that problems existed with applying the code to predict evaporation from fly ash used in the study. Some of the problems included: (1) the limitation in application caused by the algorithms and (2) the effects of the evaporation coefficient (α).

The HELP2 model was developed primarily for landfills where information on the hydraulic properties of the materials may be very limited. Due to uncertainties associated with input parameters, the algorithms used in the model were not sensitive to the strong capillary force exhibited by the ash. The code was equipped with various default parameters including; daily and monthly temperatures, solar radiation, evaporation depth, porosity, field capacity, saturated hydraulic conductivity and wilting point. The default data was based on 18 soil types and climatological data from 102 selected cities. The hydraulic properties of fly ash were unique and did not correlate well with default HELP2 soil values. Fly ash exhibited high capillary forces due to uniform grain-size distribution and small particle diameters (silt to clay-sized particles). The high capillary forces were relevant in evaporation predictions because capillary action pulls moisture up from within the soil. This effect allows more water to the surface, permitting a high evaporation rate. Because the strong capillary forces in the ash were not fully represented in the HELP2 code the model's predictability decrease and tends to underestimate evaporation.

Another discrepancy of the model was the evaporation coefficient. The range of evaporation coefficients incorporated into the HELP2 model was based on results obtained by Ritchie (1972) as discussed in Section 2.7-5. Table 1 in that section tabulates coefficients for each of the four soils tested. The model had a limited range of default evaporation coefficients (3.3 to 5.1 mm/day$^{.5}$) to avoid exceeding the range of experimental data. However, results for experiment 2 indicated that the evaporation coefficients for the Colbert and Kingston ash were much higher, in the range of 19.9 and 14.6 mm/day$^{.5}$, respectively. The evaporation coefficients determined for the experimental data for both Colbert and Kingston fly ash are shown in Appendix B, first in Table 4 and then as a series of graphs. The coefficients were determined from the slope of a straight-line fit of the cumulative evaporation versus square root of time. The HELP2 model calculated an evaporation coefficient of 5.1 mm/day$^{.5}$, which is the maximum value permitted. By definition, a higher evaporation rate is a consequence of a higher evaporation coefficient. The model only provided a range of evaporation coefficient from 3.3 to 5.1 mm/day$^{.5}$. To examine the effects of the evaporation coefficient, the code was slightly modified to incorporate higher values. The results of this analysis are shown in Appendix C.

The results of the sensitivity analyses indicated that the total evaporation was mildly affected to increases in the evaporation coefficient above 5.1 mm/day$^{.5}$. This is troublesome, because higher evaporation coefficients should result in higher evaporation rates. The evaporation coefficient should be given careful attention if the HELP2 model is to be used for predicting evaporation of fly ash.

9.1.3 WF Model

The evaporation predicted by the WF Model (for experiment 2) was approximately 6.3% less than the observed evaporation by the end of the study for the Colbert fly ash and 5.4% less for the Kingston fly ash. The results of the WF model simulation (from experiment 1) indicated that the length of the columns were underestimated with respect to moisture movement. This was revealed by examining the moisture profile. The model, based on soil physics, approximated a moisture profile as a series of blocks throughout the column. However, due to the hydraulic properties of the ash, the profile of Experiment 1 extended beyond the actual length of the cylinder. This presented an erroneous output and was not included in the analysis of the results. Also, this formed the basis for conducting an additional evaporation experiment. The comparison of actual results plotted in conjunction with modeled results from experiment 2 and represented in Figures 23 and 24 showed that reasonable evaporation simulation from fly ash was possible with the WF model.

The WF model is thought to have an anologic advantage over the other two models--that is, the model uses the hydraulic properties of the site specific material. In the evaporation study, the length of the column played an important role in evaluating the model. However, under actual field conditions, fly ash dry stacks greatly exceeded 46-cm and provided enough length to simulate a moisture profile.

However, one drawback from the model was the accuracy and amount of information needed to perform a simulation.

The model required knowledge of the hydraulic properties $K(\theta)$ and $D(\theta)$ and assumed $D(\theta)$ was either a power or an exponential function. It also required a meteorological data base comprised of rainfall and PE rates. In actual field conditions the climatological data required is often based on historical averages, and measurements of hydraulic properties usually required extensive laboratory analysis. Another factor to consider is that the model was highly sensitive to the initial moisture content and assumed the moisture profile was uniform. Any deviation in the initial moisture content could result in inaccurate predications.

10.0 Conclusion

The results from the column evaporation study show that the Wetting Front model can accurately predict evaporation of moisture in fly ash. It more accurately predicts evaporation because it is derived from the Richard's equation and is not based on default soil data. For the three models evaluated (UNSAT1D, HELP2 and WF model), only the wetting front model had algorithms capable of describing the hydraulic properties of the ash based on suction and moisture relationships. The suction-moisture relationships for HELP2 are not required, since water is only removed from the evaporative depth. The suction-moisture relationships for UNSAT1D are based on field experiments for particular soil types that do not correspond with fly ash.

Data from the study that appear to affect the performance of the HELP2 and UNSAT1D model include: (1) the evaporation coefficient, (2) potential evaporation, and (3) first and second stage evaporation. These parameters are helpful and informative in the evaluation of the models and can be used to further describe fly ash, since limited information on moisture movement and evaporation rates exist.

All three parameters affect the models in different ways. HELP2 is the only model that uses the evaporation coefficient. This coefficient, represented as α, has lower and upper limits of 3.3 and 5.1, respectively. These limits do not correspond with actual limits experimentally derived for fly ash, shown in Table 4. The evaporation coefficients for Colbert fly ash range an order of magnitude are higher than the default limits used by HELP2. Kingston fly ash values also show similar differences, ranging from 14.6 to 43.5 $(mm/day)^{1/2}$.

All three models use the potential evaporation as input data. HELP2 calculates the potential rate internally based on input parameters, while UNSAT1D has the option of calculating the potential or having the value input directly. The value for potential evaporation of the ash, used in the model was approximately .88 cm/day. This value was based on the potential evaporation rate of a free water surface. Assuming that the surfaces of the ash and the free-water experience similar evaporative demands. Since this assumption was not validated, additional evaporation tests were conducted to check for differences. These tests indicated that both potentials were the same and the assumption was correct.

The drying of soils as a result of evaporation has been documented as having occurred in two distinct stages. In the first stage, sometimes referred to as the constant-rate stage, it remains constant and is equal to the potential evaporation. During the second stage, the drying rate decreases with time and is dependent on the unsaturated hydraulic properties of the soil. This concept of staged evaporation is thought to occur in fly ash as well, but, has not been verified by conclusive literature.

The experiment conducted on the ash columns showed that Colbert and Kingston fly ash experienced first-and second-stage evaporation. This was determined by the change in slope shown in the evaporation curves. The results of the study show that length of stage I is dependent on the initial moisture content of the material. Once the evaporation rate of the ash is no longer equal to the potential evaporation rate the drying process is considered to be stage II. During stage II evaporation, the amount of moisture removed from the ash decreased with time. This decrease implies that the evaporation rate becomes independent on the potential evaporation and dependent of the water content distribution and moisture transmitting properties of the ash. Since the evaporation rate of the ash varies with moisture content and the water transmitting properties of the ash, it is recommended that any model used to simulate the evaporation process should, also, show similar effects (i.e., simulate first and second stage drying).

For the three models used in the evaluation only two of the models (WF and HELP2) have algorithms for first and second stage evaporation. UNSAT1D assumes transpiration is the principal mechanism for the transfer of soil-water to the atmosphere.

Based on the results of the study, it is recommended that the Wetting Front model or a model derived from the Richard's equation be selected to conduct modeling applications on fly ash. Since design success and improvement of dry stacks are evaluated on the amount of leachate qualities produced, an accurate assessment of the water budget must be carried out.

BIBLIOGRAPHY

BIBLIOGRAPHY

Aslying, H. C., 1963, Report Commission I. Soil Physics Terminology. Bulletin of the International Society of Soil Science, No. 23, pp. 7-10.

Beese, F., R. R. Van Der Ploeg and W. Richter, 1977, "Test of a Soil Water Model Under Field Conditions," Soil Science Society of America Journal, 41:979-984.

Bond, F. W., and G. W. Dawson, 1987, "UNSAT1D Groundwater Computer Code Manual: IBM PC version," EPRI Report CS-5512-CCML, Electric Power Research Institute, Palo Alto, CA.

Brooks, R. H., and A. T. Corey, 1964, "Hydraulic Properties of Porous Media," Hydrology Paper 3, Colorado State Univ., Fort Collins, co.

Brutsaert, W., 1982, Evaporation Into the Atmosphere, Theory, History and Applications, D. Reidel Pub., London, England.

Buckingham, E., 1907, "Studies of the Movement of Soil Moisture," U.S. Dept. Agr. Bur. Soils Bull., No. 38.

Campbell, G. S., 1974, "A Simple Method for Determining Unsaturated Hydraulic Conductivity From Moisture Retention Data," Soil Sci., 1176:311-314.

Childs, E. C., and N. Collis-George, 1959, "The Permeability of Porous Materials," Proc. Roy. Soc., A201, pp.392-405.

Chow, Ven Te, D. R. Maidment, and L. W. Mays, 1988, Applied Hydrology, McGraw-Hill.

Clapp, R. B. and G. M. Hornberger, 1978, "Empirical Equation for Some Soil Hydraulic Properties," Water Resources Research, Vol. 14, No. 4, pp. 601-604.

Clapp, R. B., 1982, "A Wetting Front Model of Soil Water Dynamics," Ph.D. Dissertation, Dept. of Environmental Science, University of Virginia, Charlottesville, Va.

Clapp, R. B., 1983, "The Continuous Similarity Model of Bulk Soil-water Evaporation," AgRISTARS, Tech. Rept. No. CP-53-00417, Remote Sensing Systems Laboratory, Dept. of Civil Engin., Univ. of Maryland, College Park, MD.

Crank, J., 1975, The Mathematics of Diffusion, 2nd ed., Oxford University Press, New York.

D. B. Stephens & Associates, Inc., 1989, "Laboratory Analysis of Hydraulic Properties of Kingston and Colbert Fly Ash."

Freeze, R. A., and J. A. Cherry, 1979, Groundwater, Prentice-Hall, Inc., New York. pp. 605.

Fribourg, H. A., 1976, "Solar Energy Variability at Knoxville TN," TN Farm and Home Science, 3:24-27.

Gupta, S. K., K. K Tanji, D. R. Nielsen, J. W. Biggar, C. S. Simmons, and J. L. Macintyre, 1978, "Field Simulation of Soil-water Movement With Crop Water Extraction," University of California, Department of Land, Air and Water Resources Water Science and Engineering Paper No. 4013.

Gardner, W. H. and J. C. Hsien, 1956, "Water Velocity in Unsaturated Porous Materials," Soil Science Society Proceeding, pp. 157-161.

Gardner, W. R., D. Hillel, and Y. Benyamini, 1970, "Post Irrigation Movement of Soil Water: II, Simultaneous Redistribution and Evaporation," Water Resour. Res., 6:1148-1153.

Green,W. H., and C. A. Ampt, 1911, "Studies in Soil Physics, I, Flow of Air and Water Through Soils," J. Agr. Sci., 4:1-24.

Hausenbuiller, R. L., 1972, Soil Science Principles and Practices, W. M. C. Brown Company Publishers, Dubuque, Iowa.

Hillel, D., 1971, Soil and Water: Physical Principles and Process, Academic Press, New York.

Kaluvachchi, J. J. and J. C. Parker, 1987, "Effects of Hysteresis With Entrapment of Water Flow in the Unsaturated Zone," Water Resources Research, 12(10):1967-1976.

Klute, A., 1952, "A Numerical Method for Solving The Flow Equation for Water in Unsaturated Materials," Soil Sci, 73:105-116.

Klute, A., 1972, "The Determination of the Hydraulic Conductivity and Diffusivity of Unsaturated Soils," Soil Sci, 113:264-276.

Knisel, W. J., Jr., Editor, 1980, "CREAMS: A Field Scale Model for Chemical Runoff and Erosion From Agricultural Management System," Vols. I, II, and III, Draft Copy, USDA-SEA, Conservation Service Report 26, pp. 643.

Markar, M. S., and R. G. Mein, 1987, "Modeling of Evapotranspiration From Homogenous Soils," Water Resources Research, 23(10):2001-2007.

Mualem, Y., 1976a, "A New Model for Predicting the Hydraulic Conductivity of Unsaturated Media," Water Resources Research, 12(3):513-522.

Philip J. R., 1972, "Future Problems of Soil Water Research," Soil Sci, 116:294-300.

Richards, L. A., 1931, "Capillary Conduction of liquids Through Porous Media," Physics, 1(4):318-333.

Ritchie J. T. and E. Burnett, 1971, "Dryland Evaporative Flux in a Subhumid Climate, 2, Plant Influences," Agrom. J, 63:56-62.

Ritchie J. T., 1972, "Model for Predicting Evaporation From a Row Crop With Incomplete Cover," Water Res. Res., 8(5): 1204-1213.

Royer, J. M. and Vachaud, G., 1975, "Field Determination of Hysteresis in Soil-water Characteristics," Soil Sci. Soc. Am, 39:221-223.

Schroeder, P. R., B. M. McEnroe and J. Sjostrum, 1988, "Hydrologic Evaluation of Landfill Performance Model (Version 2)," Draft Report, U.S. Army Engineer Waterways Experiment Station, Vicksburg, MS.

Skaggs, R. W., and R. Khalael, 1982, "Infiltration, Chapter 4, Hydrologic Modeling of Small Watersheds," American Society of Agricultural Engineers, Monograph No. 5, pp. 121-168.

Skaggs, R. W., 1982, "Hydrological Modeling of Small Watersheds," ASAE.

Van Bavel, C. H. M. and D. I. Hillel, 1976, "Calculating Potential and Actual Evaporation From a Bare Soil Surface by Simulation of Concurrent Flow of Water and Heat," Agric. Meteorol., 17:453-476.

USDA, 1972, Soil Conservation Service: National Engineering Handbook. Section 4, Hydrology, U.S. Government Printing Office, Washington, D.C.

Viessman, W., J. K. Knapp, G. L. Lewis, T. E. Harabaugh, 1977, Introduction to Hydrology, Harper and Row.

Young, S. C., and L. M. Beard, 1989, "An Assessment of the Phase II Fly Ash Dry Stacking at the Bull Run Fossil Plant," Report No. WR28-1-49-104, Tennessee Valley Authority, Engineering Laboratory, Norris, TN.

Young, S. C., 1989, "Leachate Generation From Dry Stacking Fly Ash at the Bull Run Fossil Plant, Part I: Field Experiments, Report No. WR28-1-49-102, Tennessee Valley Authority, Engineering Laboratory, Norris, TN.

Appendices

Appendix A

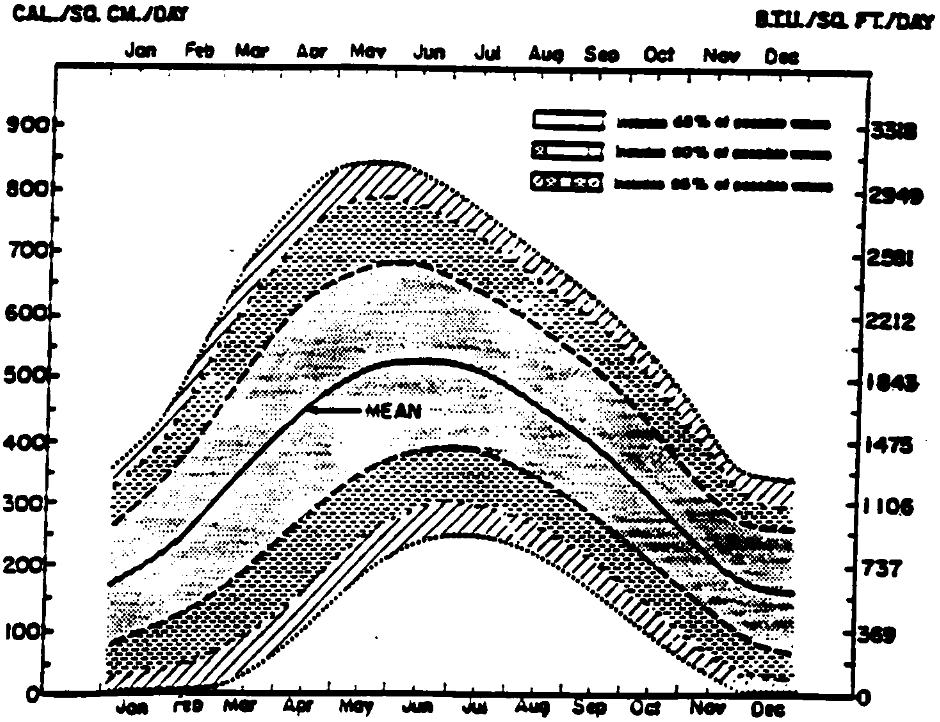

Figure 2. Fitted curves for daily solar radiation at Knoxville, 1960-1975, and for daily means plus or minus 1.0, 1.64, or 2.0 s.

Tennessee Farm and Home Science

Appendix B

The evaporation coefficient of fly ash for the different moisture contents was not compared until the evaporation tests were finished. The results for Colbert and Kingston fly ash are shown in Table 4, then by the following graphs.

Table 4. Evaporation Coefficients Derived from the Experimental Study

Colbert and Kingston Evaporation Coefficients			
Colbert Fly Ash		Kingston Fly Ash	
Moisture Content (%)	Evap. Coeff. ($mm/day^{1/2}$)	Moisture Content (%)	Evap. Coeff. ($mm/day^{1/2}$)
43	21.9	35	16.9
24	19.9	22	14.6
near saturation	47.2	near saturation	43.5

EVAPORATION COEFFICIENT
EXPERIMENT I COLBERT FLY ASH

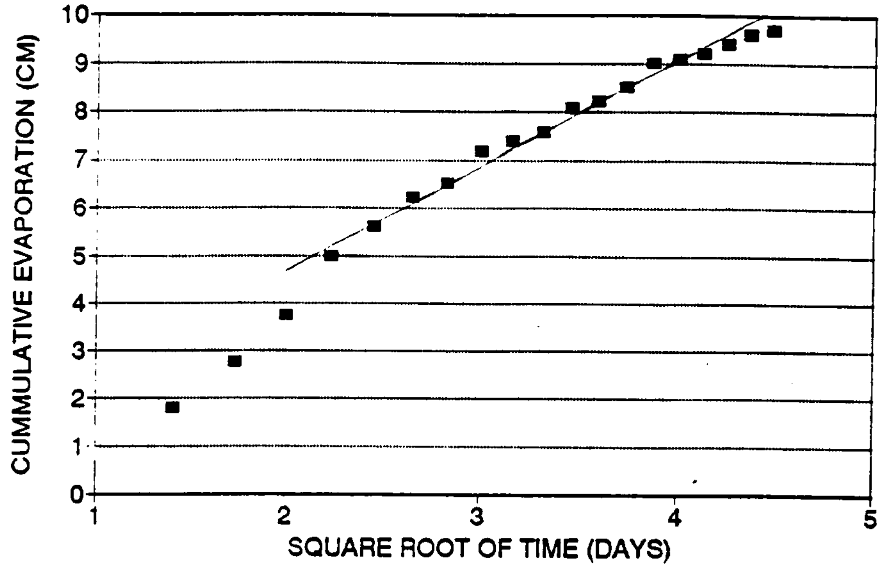

Moisture content (%)	Evaporation coeff.(mm/day$^{1/2}$)
43%	21.9

EVAPORATION COEFFICIENT
EXPERIMENT II COLBERT FLY ASH

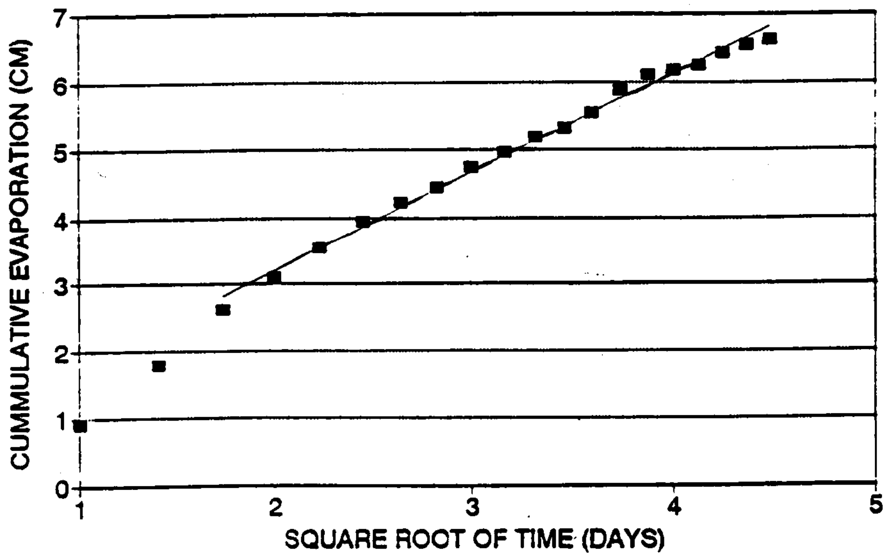

Moisture content (%)	Evaporation coeff.(mm/day$^{1/2}$)
24%	19.9

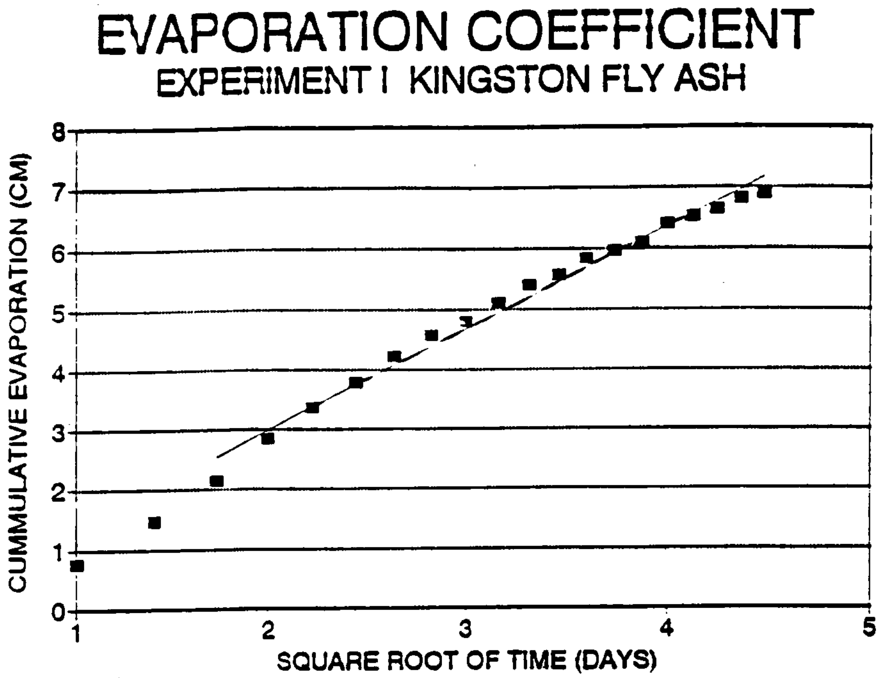

Moisture content (%) Evaporation coeff. (mm/day$^{1/2}$)
35% 16.9

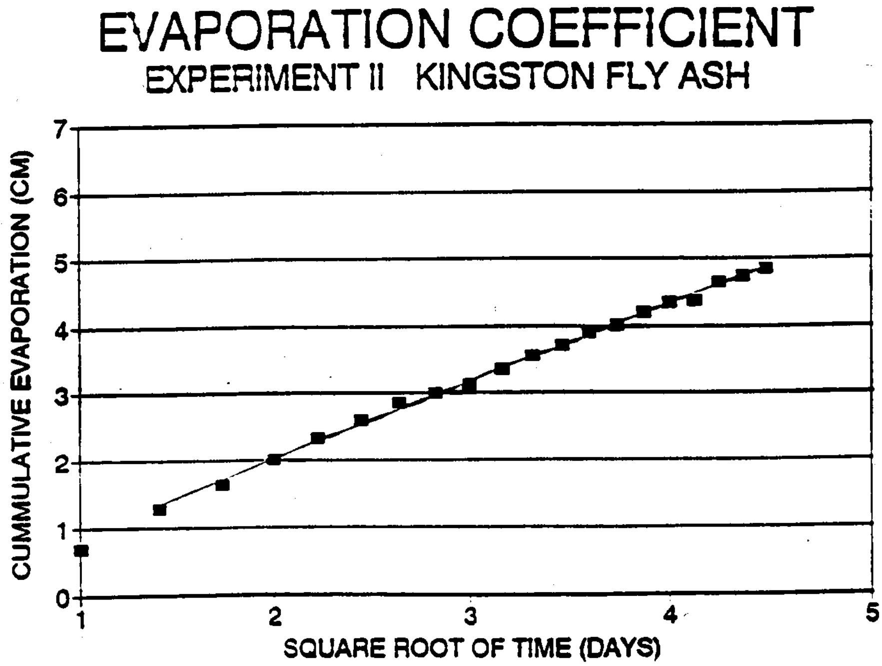

Moisture content (%) Evaporation coeff. (mm/day$^{1/2}$)
22% 14.6

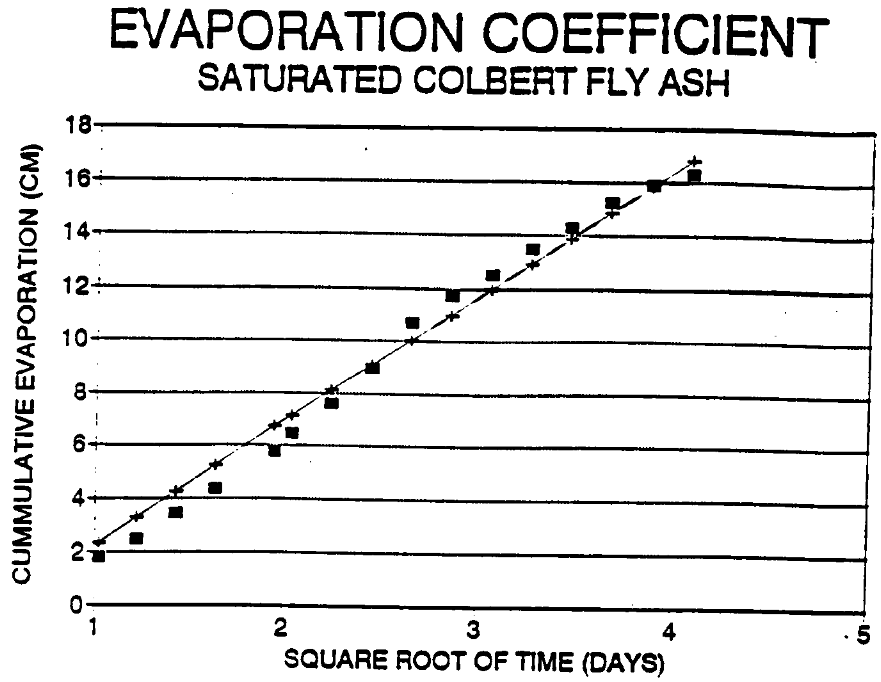

Moisture content (%)	Evaporation coeff.(mm/day$^{1/2}$)
Saturated	47.2

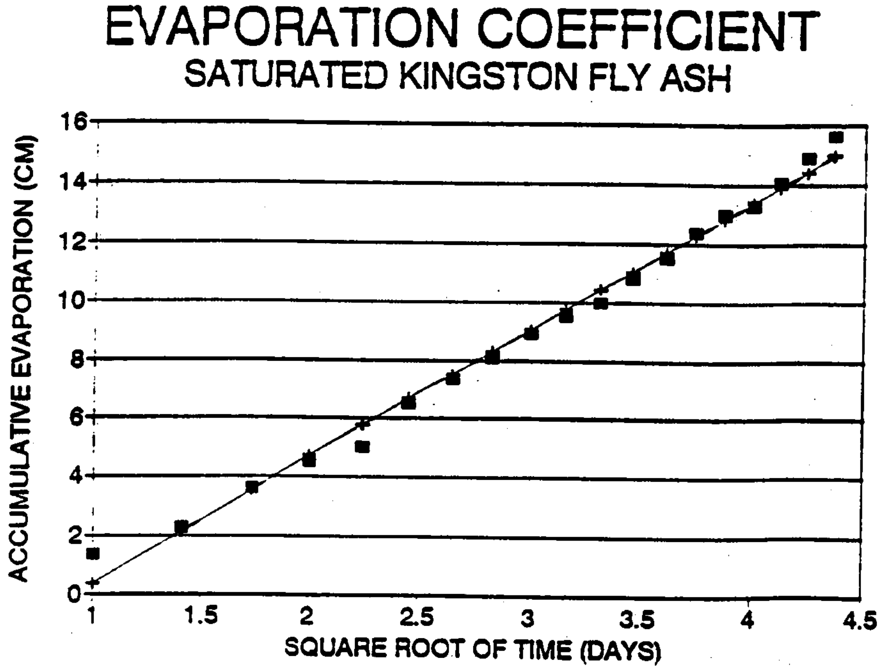

Moisture content (%)	Evaporation coeff.(mm/day$^{1/2}$)
Saturated	43.5

APPENDIX C

The HELP2 code has a built in algorithm used to determine the evaporation coefficient based on empirical equations shown in Table 1. These equations relate values of alpha to the unsaturated hydraulic conductivity at 0.1 bars. Schroeder, etal., (1988) developed these equations based on the experimental results of Ritchie (1972). Upper and lower limits are placed on the values of alpha so as not to exceed the range of the experimental data. The code was modified by bypassing the routine used for calculating the evaporation coefficient. Instead, additional statements were added to allow the input of the coefficient at the computer terminal. The code was compiled and various alpha coefficients ranging from 5.1 to 10 were used in the analyses. The sensitivity analyses results is shown on follow page.

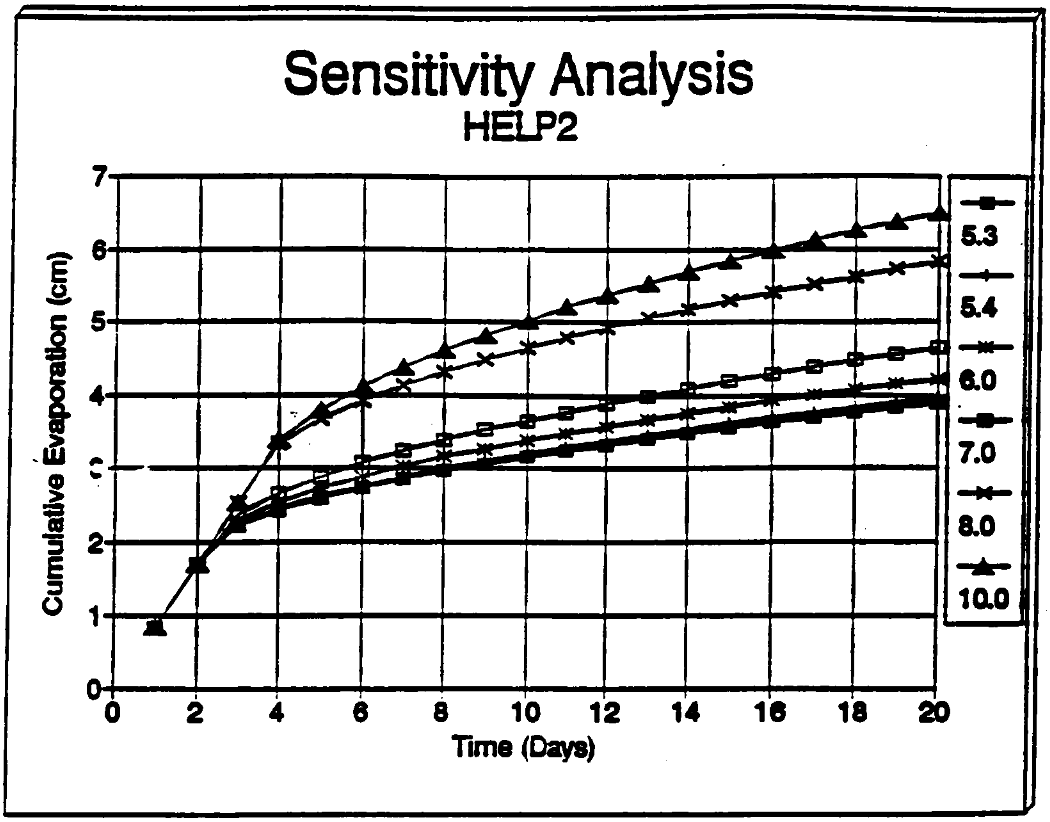

Sensitivity Analysis
HELP2
Cumulative Evaporation (cm)
Time (Days)
0
1
2
3
4
5
6
7
0
2
4
6
8
10
12
14
16
18
20
5.3
5.4
6.0
7.0
8.0
10.0

VITA

Denver Dewayne Foust was born in Knoxville, Tennessee on June 29, 1963. He lived in Maynardville and attended Maynardville public schools until graduation from Horace Maynard High School in June 1981. Approximately four years later, he entered the University of Tennessee, Knoxville, and in August 1989 received a Bachelor of Science Degree in Agricultural Engineering.

The following semester he enrolled in the University of Tennessee graduate school. While pursuing a Master's Degree, Dewayne worked as a graduate research assistant with Tennessee Valley Authority, Norris Engineering Laboratory.

In July 1991, Dewayne became a full-time employee with the Process Engineering Division of Martin Marietta Energy Systems, Inc. Requirements for a Master of Science Degree in Environmental Engineering were completed in May 1992.